Freie Universität Berlin
Departement for Geoscience
Institute for Geographical Science
Physical Geography

Carbon availability in soils of thermo-erosional valleys – a case study from a valley on Herschel Island, West Canadian Arctic

First examiner: Prof. Dr. Margot Böse

Second examiner: Prof. Dr. Hugues Lantuit

Bachelor-Thesis

Luca Durstewitz (4764040)

Wintersemster 2017/18

Berlin, 24.11.2017

Walterstraße 4
12051 Berlin
durstluca@zedat.fu-berlin.de
9. Semester

ALFRED-WEGENER-INSTITUT
HELMHOLTZ-ZENTRUM FÜR POLAR- UND MEERESFORSCHUNG

Table of Content

List of Figures

List of Tables

List of Maps

Abstract

Permafrost is a perennially frozen ground often occurring in periglacial environments. Due to its frozen state, organic carbon accumulates in the soils. By temperature rise and thaw of the active layer, these stocks become vulnerable to microbial decomposition. To predict the future of organic carbon in the Arctic, it is necessary to expand the knowledge on its spatial distribution across arctic environments. This study examined the spatial distribution of organic carbon and its availability within a valley, which is subjected to thermo-erosion on Herschel Island, Yukon Territory. By analyses of soil samples variations in soil organic carbon, total nitrogen and the carbon-to-nitrogen ratio (C/N) were investigated. Ecological units, hillslope position and distance to shore helped to identify spatial differences between sites. The analyses showed that highest values for soil organic carbon, total nitrogen and C/N occurred on uplands, followed closely of the values in the valley bed. On slopes the values of soil organic carbon, total nitrogen and C/N were lower. Further, differences of the soil organic carbon, total nitrogen and C/N stocks occurred across the valley locations with distance to the shore. Upstream the soil organic carbon, total nitrogen and C/N stocks were higher to those downstream. Sites on slopes and downstream are characterized by continuous surface disturbances due to permafrost degradation, thermo-erosion and hillslope processes. This study could demonstrate that even in local scales organic carbon stocks and its availability differs spatially depending on environmental parameters.

1. Introduction

High-latitude regions of the northern hemisphere are drastically affected by global climate change and undergo an atmospheric temperature increase with a prognosis of 3 to 8 °C by 2100 (Barry & Gan 2011: 323; Schuur et al. 2008: 702). Along the Yukon coast, the area of interest, the temperature has increased by approximately 2.5 °C during the past 100 years (Burn & Zhang 2009: 15). The rise in air temperature has a huge impact on the Arctic because these environments are characterized by the presence of ice in the ground, which strongly responds to warming and is therefore exposed to future climate changes (Pizano et al. 2014: 2; Hugelius 2011: 9). Almost 24 % of the northern hemisphere is underlain by permafrost (*figure 1*) (French 2007: 95). Permafrost is defined as soil or sediment that is frozen for at least two consecutive years. The soil top layer that thaws seasonally is termed active layer (French 2007: 85). Permafrost is sensitive to changes in air temperature and is currently thawing (Schuur 2008: 706). With increasing temperatures the active layer deepens (French 2007: 85). Since high-latitude soils store huge quantities of carbon they have a large potential impact on the global carbon cycle (Hobbie et al. 2000: 196; McGuire et al. 2009: 524), as two-third of the fossil carbon may be released into the atmosphere and partly will be dissolved in hydrological systems (Vonk et al. 2012: 137).

Low soil temperatures and poor drainage limits microbial decomposition in permafrost soils (Hugelius 2011: 9) and facilitates organic carbon (OC) accumulation especially in peatlands. This terrestrial OC is present due to biotic activity as vegetative biomass and in soil organic matter (SOM) (McGuire et al. 2009: 526). When the top layer thaws, the soil microorganism activity gets enhanced and leads to an increase in the decomposition of organic matter and to mineralization of carbon and nitrogen (Zech et al. 2014: 3).

Because of the vulnerability of permafrost soils to temperature rise, previous studies estimated the pool of soil organic carbon (SOC). Tarnocai et al. (2009) estimated a SOC amount of 1024 Pg (2009: 7) and Hugelius et al. (2014) calculated stocks of 1307 Pg stored in 0–300 cm permafrost depths (2014: 6590), which is nearly half of the global storage amount (Tarnocai 2009: 1).

Generally, the OC stocks are impacted by geomorphic disturbances. According to a study by Obu et al. (2015), the storage of OC relates to surface morphology. Along with the assessment of different storages of SOC and total nitrogen (TN), they showed that there is less SOC stored in areas that underlie higher erosion rates (Obu et al. 2015: 101). Upon thawing, arctic landscapes will be more exposed to erosional dynamics and disturbances, e.g. massive coastal

erosion and rapid mass movements such as slumps or slow mass movements like solifluction or gelifluction (Smith et al. 1989: 9; Lantuit & Pollard 2005: 413). When occurring along the arctic coast, these physical processes are responsible for an increased transportation rate of sediments into the nearshore marine environment, which contributes to modify the parameters of the carbon cycle and thereby the conditions of the regional chemistry (Jorgenson & Brown 2005: 78; Günther et al. 2013: 4298; Tanski et al. 2017: 435). Due to that here is therefore an urgent need to understand the impact of surface disturbances on the stocks of OC and TN in the Arctic.

Recent studies have attempted to discuss the impact of distribution on organic matter storage but often just focused on rapid mass movements and the related transport of organic material (Obu et al. 2015: 104). However, no study investigated the impact of one prominent geomorphic feature of the Arctic on the SOC stocks: thermo-erosional valleys (TEV) (Godin et al. 2014: 2). Thermo-erosional processes are frequent on slopes with frozen ground (Morgenstern 2012: 73). These mass wasting processes are a combination of thermal and mechanical actions (van Everdingen 2005: 80) and are closely linked to valley developments in landscapes underlain by continuous permafrost (French 2007: 193).

Within TEVs, permafrost influences the water fluxes to a great extent, since it prohibits the water to percolate into the ground and enhances the pore-water pressure, which is resulting in downslope movements such as solifluction or gelifluction and the displacement of solved substrates, such as carbon (French 2007: 224). However, the effect of erosion, terrain, hillslope positions and hillslope gradient on decomposition rates and availability within TEVs is relatively unknown.

This study aims to estimate the carbon availability in soils of a thermo-erosional valley on Herschel Island, West Canadian Arctic.

The availability of carbon depends on the qualitative and quantitative carbon presence and physical landscape processes (Weiss 2017: 7). Thaw increases carbon availability for decay and thereby exceed the decomposition processes of microorganisms (Weiss 2017: 7). For the calculation of carbon stocks and their availability it is important to know how much OC is distributed and stored on different surface terrains.

Therefore, soil samples were taken in a TEV on Herschel Island (Yukon Territory, Canada) and analyzed to measure TOC and TN, in order to explain the variability in the carbon-to-nitrogen ratio (C/N) and relate it to geomorphic disturbances within a valley.

2. Background

2.1. Permafrost and Periglacial Environments

Permafrost is confined to high latitudinal terrestrial and marine regions or to elevated mountain ranges (*figure 1*) (Ehlers 2011: 187; Barry & Gan 2011: 167). It can consist of ice rich ground material and/or sediments (rocks), organic matter and ice, which remains at or below 0 °C for at least two consecutive years (van Everdingen 2005: 55; Ehlers 2011: 185; French 2007: 84). Permafrost gets classified in accordance to its extent in a landscape. If more than 90 % is underlain by permafrost it gets referred to 'continuous permafrost', areas with a lower extent are summarized as 'discontinuous permafrost' (French 2007: 94).

Most of the current permafrost formed during the last glaciation period (Fritz 2011: 27; Barry & Gan 2011: 178) and presently underlays about 36.2 million km² globally (French 2007: 95).

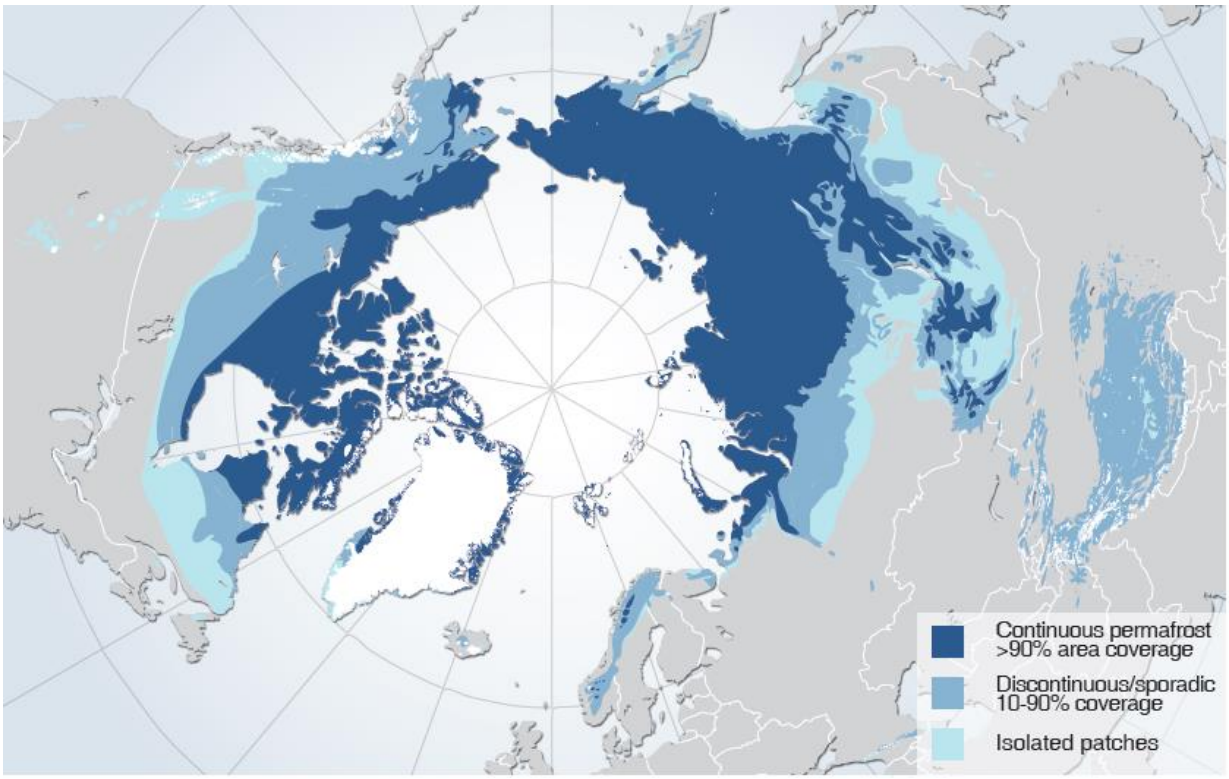

Figure 1: Thematic map of the circum-polar permafrost extent.
(obtained at: http://www.grida.no/graphicslib/detail/permafrost-extent-in-the-northern-hemisphere_1266#, accessed 14. October 2017; by Hugo Ahlenius, UNEP/GRID-Arendal; modification of Brown et al., 1997)

In Siberia, the continental climate conditions and the partly glaciated mountain regions enabled an important development of ground ice (French 2007: 98), whereas the glacial regression of the massive ice shield in North America created a landscape characterized by enormous quantities of meltwater and a great distribution of post-glacial lakes, which partially prohibited ground ice to grow (French 2007: 98). Because of this, the North American region shows, on a global scale, only the second largest amount of frozen ground with a

contemporary spatial extent of 5.7 million km² (Ehlers & Gibbard 2007: 13; French 2007: 84) behind the Siberian region (French 2007: 98; Ehlers 2011: 185).

2.2. Permafrost Degradation and main Periglacial Landforms

In periglacial environments, ground-ice and permafrost strongly influence the landscape (Barry & Gan 2011: 183). As soon as ground ice melts, it modifies ground conditions. Unconsolidated sediments made cohesive by ice, get easily eroded and therefore are highly vulnerable to temperature rises (Lantuit & Pollard 2008: 86; Ehlers 2011: 185). Permafrost degradation starts by continuous deepening of the active layer, resulting in subsurface and surface water concentrations (Schaefer et al. 2014: 3). As soon as water bodies (such as thaw lakes and streams) get more common in these environments the local heat transfer in the ground get changed, creating specific landscape features linked to a combination of thermal and/or gravity induced mechanical actions. These degradation processes are defined as thermokarst and thermo-erosion (Morgenstern 2012: 74; Lantuit & Pollard 2005: 415). Thermokarst occurs by thaw of ice-rich ground that can cause *in situ* surface subsidence due to a loss of volume (French 2007: 191), forming typical polygonal structures and a high distribution of lakes. Thermal erosion on the other hand, is combined by thermal actions (i.e., thaw) and mechanical actions (i.e., transportation) ablating unconsolidated frozen sediments (Morgenstern 2012: 74; Günther et al. 2012: 137). This dynamic process of permafrost degradation often occurs on coastlines and river banks, as well as in landforms with small reliefs formed by initialed water runoff. Both processes can be intensified by an increasing depth of the active layer and can cause the release of fossil OC (Morgenstern 2012: 73).

Landscapes that are subject to permafrost degradation and high erosion rates will be summarized to ‘disturbed’ landscapes in this study. Areas of low degradation or erosion rates will be generally named ‘undisturbed’ terrains.

2.3. Carbon Stocks

SOC stocks in arctic permafrost soils are 1300 Pg within a depth of 300 cm. Just 800 Pg is assumed to be frozen for several years (Hugelius et al. 2014: 6590). In comparison, global SOC storages were estimated to 2376–2456 Pg for 0–200 cm depth and 351 Pg (200–300 cm) (Tarnocai 2009: 1). These numbers demonstrate that a major part of OC stocks is located in arctic regions (Davidson & Janssens 2006: 165; Tarnocai 2009: 7).

SOC that is stored in permafrost plays a major role in predicting climatic changes due to temperature rise because it is a source of greenhouse gases (such as carbon dioxide and methane), which get emitted by microbial activity (Schaefer et al. 2014: 2). The rise in temperature causes the organic material to again become subject to mineralization and decomposition by microbes after being protected by conditioned ground temperatures of 0°C (Davidson & Janssen 2006: 167).

Even though the biomass production in high-latitude areas is low, tundra soils are known for their high organic soil content (Zech et al. 2014: 3). Arctic SOC stocks are high due to a hindered microbial activity related to cold temperature, poorly drained conditions and anoxic soil conditions. (Zech et al. 2014: 3; Hugelius et al. 2012: 1; Pizano et al. 2014: 2; Strauss et al. 2015: 2228).

Moreover, the soils are subject to cryoturbation that enables deposition of organic matter into deeper soil layers and limits the decomposition of the organic matter (Lantuit et al. 2012: 392; Hobbie et al. 2000: 200). But in coming decades much of the organic-rich, arctic and subarctic soils preserved from thawing for millennia could become subject to degradation and mineralization (Hugelius et al. 2014: 6574; Tanski et al. 2017: 435); and with a thickening of the active layer the decomposition rate rises and greenhouse gases get released (Hugelius et al. 2014: 6574).

This could impact the earth system by a presumed potential temperature rise of 0.29 ± 0.21 °C until 2100, just induced by CO_2 and CH_4 emissions of permafrost degradation (Schaefer et al. 2014: 7).

2.4. Soil Organic Matter Decomposition

Soil organic matter (SOM) is the accumulative fraction of the uppermost soil layer mainly provided by plant detritus, leafs, roots or charcoal (Meyers & Teraines 2001: 239) and is the main product for microbial metabolism (*figure 2*). The biochemical degrading process is generally known as soil respiration, which is directly linked to the atmosphere (White 2013: 565). The mineralization of organic plant-based decay by soil unicellular microorganisms plays a key role in the nutrient cycle (White 2013: 565).

Organic matter underlies microbial decomposition (White 2013: 565), whereby carbon gets partly incorporated into the microbial tissue and excretes CO_2 (Stevenson 1994: 100). During the degradation, the organic form of N gets transformed to NH_3 by cell synthesis (Stevenson 1994: 100).

For the decay process the convertibility depends on substrate quality for example chemical and physical structures of organic litter as well as climate, vegetation and moisture (Graham 2012: 710; Hobbie et al. 2000: 197). Lignin, soluble carbohydrates and vascular plants have a more stable structure and are therefore more difficult to decompose, leading to a limited availability of carbon and nitrogen constituents for microorganisms (Jansson & Persson 1982: 241; Hobbie 2000: 197). The C/N ratio is used as a proxy to visualize the rate of biochemical degradation of organic material within a soil profile. The ratio can also give hints on the turbation rate and accumulation of organic matter in the depths of frozen soils. With changing conditions, these parameters may alter the presence and availability of organic matter for decomposition (Weiss 2017: 7). The availability of OC is mostly attributed to its accessibility for microbial decomposition. SOM and OC in periglacial environments are fragile components of the carbon cycle that is influenced by surrounding conditions (Weiss 2017: 7). Its bioavailability, therefore, depends on predominant vegetation types, impacting the quality of organic matter, and also on the dynamic of regional landscapes (Weiss 2017: 7). Thus, enhanced thaw will increase the availability of SOM (Weiss 2017: 7).

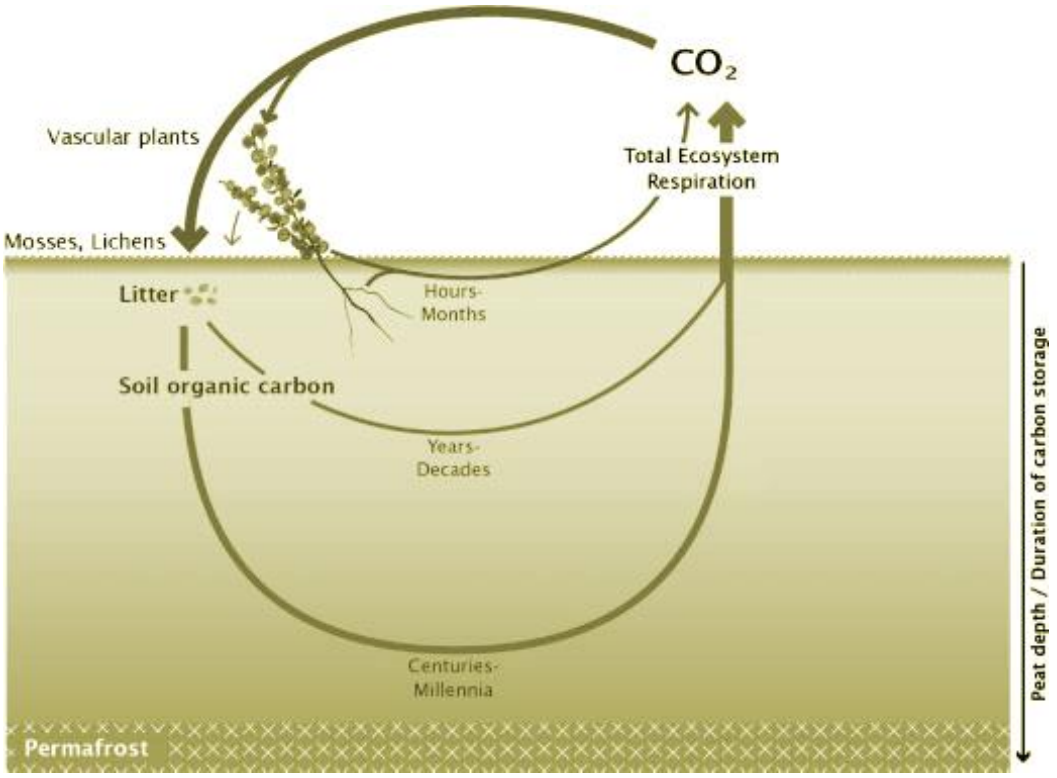

Figure 2: Schematic carbon cycle in permafrost underlain landscapes (adapted from Kuhry et al. 2010).

2.5. Thermo-erosional Valleys

In continuous permafrost environments thermo-erosional valleys (TEV) are a frequent type of periglacial degradation (Godin et al 2014: 1). These mass wasting processes are a combination of thermal and mechanical actions that occur on slopes (van Everdingen 2005: 80; Morgenstern 2012: 73). A created heat transfer by seasonally thaw and water runoff deepens the active layer of the soil subsurface (Morgenstern 2012: 73; Harms et al. 2014: 300; French 2007: 260). This results in an interplay of ground-ice loss and mechanical erosion that provokes ground subsidence and gullying (Harms et al. 2014: 300). These induced erosional mechanisms by thaw in unconsolidated grounds highly influence the valley developments in landscapes underlain by continuous permafrost (French 2007: 193).

Depending on the slope gradient and surface substrate, thermal erosion can occur as slow mass movements (Godin et al. 2014: 2; Ehlers 2011: 187) provoked by gullying and surface runoffs (van Everdingen 2005: 80). Due to the frozen state, water is prohibited to percolate into the ground. The increasing water content within the active layer exceeds the thermal equilibrium, which results in downward sliding sediment masses along the permafrost table (French 2007: 186). Destabilized landscapes with TEVs are common in arctic regions (Pizano 2014: 2; French 2007: 224; Smith et al. 1989: 9) and locally have a substantial impact on water, sediment, and organic matter transport from permafrost uplands to coastal waters (Morgenstern 2012: 74).

Generally, a TEV is formed by an accumulation of water along ice wedges that can be originated by thaw or precipitation that evokes further thaw (French 2007: 191). This results in small gullies and incise the ground by vertical and horizontal erosion undercutting collapse exposed organic soil mats (French 2007: 191). Once gullying started soil degradation and deportation is initialed (Poesen et al. 2003: 115). TEV are often asymmetric, typically, also in subarctic regions, the north-facing slope is steeper (French 2007: 263). The opposite slope is therefore characterized by a deeper active layer due to stronger solar radiation, which enables greater mass movements that lowers the slope inclination (French 2007: 263). Due to the valley asymmetry, TEVs also play an important role as niches for snow accumulation (Morgenstern 2012: 75).

Near surface sediment movements often arise during late summer when the active layer is deepest (Smith et al. 1989: 7). Depending on surface substrates, vegetation coverage (Ehlers 2011: 195) the seasonal freeze and thaw mass movements might vary in intensity (French 2007: 224).

Processes involved in TEV development are still not completely understood. Valley asymmetry shows a complex interplay of channeling and mass movements (French 2007: 248), which impact the deposition and decomposition rate of organic matter within a valley.

3. Study Area: Herschel Island

3.1. Geographical and Geological Background

Qikiqtaruk, Herschel Island (69.57N 138.91W), is situated in the southeastern arctic Beaufort Sea (*figure 3*). The island is positioned 3 km north of the Canadian mainland and approximately 100 km west of the Mackenzie Delta (Fritz et al. 2011: 27). Its geographical extent is ca. 116 km² with an elevation maximum up to 183 m.a.s.l. (Burn 2012: 30).

In 1959, Mackay proposed that Herschel Island was formed by glacial ice-thrusting (Smith et al. 1989: 4). A lobe of the Laurentide Ice Sheet advanced to the northwest of the island during Late Wisconsin Glaciation (around 23 to 18 ka BP) and upthrusted sediment from the Yukon Coastal Plain (Mackay 1959: 20; Fritz et al. 2011: 27; Lantuit & Pollard 2008: 87). During that time, the ice masses formed a push moraine of frozen continental shelf sediments (Smith et al. 1989: 5). Simultaneously a depression southeast of the ridge got scraped, which is nowadays called Herschel Basin (Smith et al. 1989: 5; Burn 2012: 33).

Because of the trajectory of the ice push, the ground dominantly contains marine and beach fine silty and sandy sediments, respectively, which got covered by glacial deposits consisting of clay, silt and sand (Burn 2012: 33; Lantuit & Pollard 2008: 87).

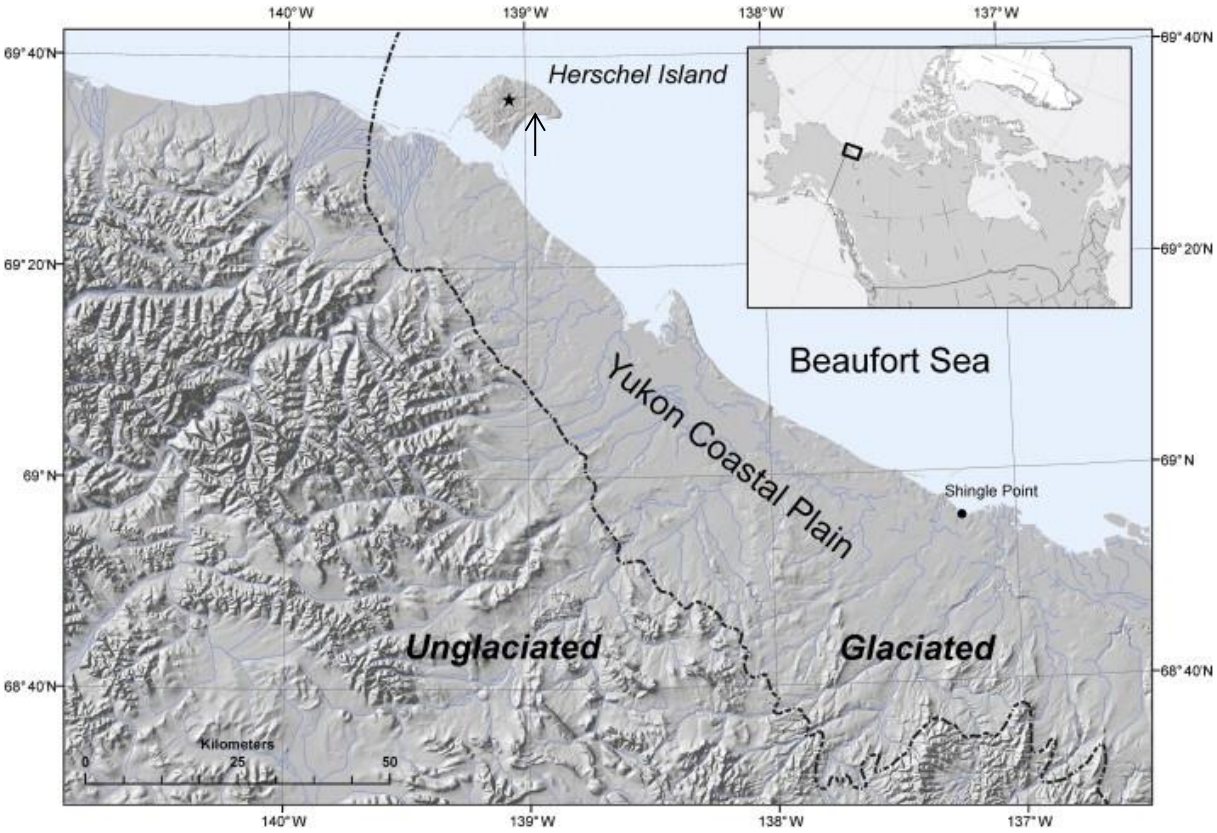

Figure 3: Location of study area Herschel Island in the West Canadian Beaufort Sea. Herschel Island is marked with a star and the study site, Fox Creek valley, is signified with an arrow. Dashed line visualizes limit of the last glaciation phase Lenz et al. 2013, modified).

3.2. Climate

Due to its high-latitude, the climatic conditions on Herschel Island are arctic by nature and is defined as polar tundra (ET) or Meadow tundra (Lantuit & Pollard 2005: 421).

The surrounding sea surface is covered during nine to ten months by sea ice reaching to the coastline (Barry 1993: 46). Consequently, the climatic conditions are moderated by the Beaufort Sea and its expansion cycles of sea ice (Burn 2012: 48). While in summer the land masses get warmed and the mean temperature rises above 5 °C; in winter, the unfrozen water column underneath the sea surface ice releases stored heat and the mean temperature decreases to a value below -25 °C (Burn 2012: 48). The mean annual temperature on Herschel Island is -9 °C (Burn 2012: 49).

On average, the annual precipitation rate is around 166 mm, whereby a half of the precipitation falls as rain during the summer months (Burn 2012: 50). Generally, the snow cover is lower than on the mainland due to a smaller amount of vegetation, which can prevent the snow from getting blown out by strong northwesterly winds (Lantuit & Pollard 2008: 96). Nonetheless, in wind sheltered valleys snow banks can accumulate some meters deep (Burn 2012: 50).

3.3. History of Settlement

Archeological evidences indicate a long-lasting settlement history of humans for the Canadian arctic territories since approximately 10 ka BP (Friesen 2012: 146). On Herschel Island Inuvialuit settlements can only be traced back eight centuries (Burn 2012: 145). During this time, the island was already separated from the mainland (Burn 2012: 145).

Physical conditions on Herschel Island and the nutrient rich Beaufort Sea offered a lucrative life for several inhabitant groups during the settlement history (Burn 2012: 6). After a long period of aboriginal occupation, in 1826 the first Euro-Americans entered the territories by discovery expeditions (Burn 2012: 7). Through the expansion of whaling, the Beaufort Sea simultaneously gained in economic interest and whale hunters stationed on the island (Burn 2012: 7). After the whale stocks collapsed in the early 20th century, the installed housings in the eastern part of the island became a police detachment (Smith et al. 1989: 3). In 1987 Herschel Island got included to a Territorial Park (Myers-Smith et al. 2011: 611).

Thanks to the history of settlement of this remote place, Herschel Island provides satisfying documentations on the surrounding environment for approximately 100 years, which makes it an interesting place for arctic research (Myers-Smith et al. 2011: 611).

3.4. Geomorphology

Herschel Island is underlain by massive frozen ground that provides cohesion to the sedimentary material (Lantuit & Pollard 2008: 87). The permafrost reaches down to presumably 450 m (Burn 2012: 67). The soil top layer annually thaws to a depth of 40 to 60 cm (Burn & Zhang 2009: 14; Burn 2012: 33). Primarily, Herschel Island shows an undulating hilly landscape that is characterized by morphological features attributed to permafrost and its degradation implying ground disturbances, subsidence processes and the instability of ground surface (Ehlers 2011: 185; French 2007: 186; Fritz et al. 2011: 26; Tanski et al. 2017: 435).

Herschel Island underlies strong coastal erosion processes with an annual retreat of 0.68 m/a^{-1} (Obu et al. 2016: 9). Numerous retrogressive thaw slumps and the exposition of massive ground ice triggers rapid landmass erosion along the south-eastern coast (Lantuit et al. 2005: 414; Pollard et al. 2012: 72; Obu et al. 2016: 3). Along the northern and western shorelines coastal retreat is dominant, eroding high bluffs reaching up to 50 m (Obu et al. 2016: 3).

The south and east coasts are characterized by a slightly hilly earth surface, shallow valleys and alluvial fans or accumulation spits (Pollard et al. 2012: 72-74; Tanski et al. 2017: 435). Polygonal nets formed by numerous merging ice wedges in poorly drained tundra are present on the upland plateaus (Ehlers 2011: 197; Smith et al. 1989: 7). These polygon tundra patterns

develop trough ground subsidence because of volume loss during the thawing season. By a refreezing of water lenses at the permafrost table pushs up small hummocks that are trapped by ice wedges (French 2007: 186; Lewellen 1970: 1).

Another frequently occurring characteristic erosional process on Herschel Island is thermal erosion (Lantuit & Pollard 2008: 86), enhancing the erosional processes on the upland by repeated changes in water saturation. Active layer thaw, snow melt, run-off and summer precipitation enforces the formation of sinkholes and tunnels that arise in downwards gulling, forming a relief of TEVs (Godin et al. 2014: 2; French 2007: 191; Smith et al. 1989: 7). Even on gentle slopes (at least 2°) continuous slow mass movements are witnessed, such as frost creep recognizable by lobes along the slope, initialed by periodical freeze and thaw (Smith et al. 1989: 9).

All these downslope movements and material loss affect the ability of the slow soil formation in tundra (Smith et al. 1989: 14). The short weathering season and cryoturbation, which enables an accumulation of organic matter in lower soil depths, blur the soil horizons (French 2007: 80; Smith et al. 1989: 9) and affects the vertical distribution of organic matter within a soil profile. On Herschel Island the organic matter content has been observed to be the highest in the active layer and the uppermost parts of the permafrost layer by values between 3 – $25_{wt\%}$ (Kokelj et al. 2002: 175).

3.5. Vegetation

The vegetation on Herschel Island is sparse due to the local arctic climate conditions of low precipitation, cold annual mean temperature and a thin active layer (Kennedy 2012: 80). Low tundra vegetation composition dominates (Myers-Smith et al. 2011: 611), with small shrubs, sedges and grasses that are able to resist the weak tundra soil development (Lewellen 1970: 1). Nevertheless, about 200 species were inventoried (Kennedy 2012: 80). The vegetative canopy is mainly represented by tussock cotton-grass (*Eriophorum vaginatum*), tundra typical shrubby dwarf willows (*Salix pulchra, Salix arctica, Salix glauca, Salix richardsonii*), various forb herbaceous species, mosses and as well graminoid species such as sedges and grasses (Myers-Smith et al. 2011: 611; Kennedy 2012: 81). With regard to different geomorphology, soil properties and moisture, the vegetation composition changes substantically i.e., on slopes these changes can easily be observed (Kennedy 2012: 82).

3.6. Ecological Units

Smith et al. (1989) defined ecological units on Herschel Island based on a detailed survey on soils and vegetation types and linked this classification to specific geomorphological terrain. In later studies (Obu et al. 2015; Myers-Smith et al. 2011; Burn & Zhang 2009), these ecological units were often used to subdivide terrain and calculate changes within it. This research also takes advantage of the ecological classification as an overarching framework to characterize organic matter storage, its spatial distribution and quality within TEVs. Along the study sites following units appear (*map 2*):

- *Guillemot* describes areas of wet ice wedge-polygonal ground or depressions with standing water and occurring channels. Peat accumulation, counting several decimeters above mineral soil, is common (Siewert, 2016: 4; Smith et al. 1989: 41),
- *Herschel* describes uplands and gentle slopes with dense vegetation and common tussock tundra on a micro-hummocky surface with a shallow active layer (Siewert, 2016: 4; Smith et al. 1989: 44),
- *Komakuk* as the most common unit type on Herschel Island describes uplands and moderate slopes (7 %) with discontinuous vegetation coverage and exposed soil. The soils are fine-textured and mostly well drained, in wetter soils especially cotton grass and mosses dominate the vegetation composition, whereas the vegetation in well drained ground is normally characterized by arctic willow (Siewert, 2016: 4; Smith et al. 1989: 49),
- *Plover* unit is mostly occurring on gently convex sloping terrain or crests with >40% bare soils exposure by degradation and erosion. Cryoturbation within the soils is common. The vegetative coverage consists predominantly of Willow/Dryas-Vetches (Smith et al. 1989: 52),
- *Jaeger* represents moderate erosion across heterogeneous slope surfaces with different vegetation circles du to varying soil moisture. (Smith et al. 1989: 46).

In this study the Plover and Jaeger unit is combined as in the study of Obu et al. (2015). *Table 1* shows the geomorphological, pedological and biophysical parameters associated with the relevant ecological units compiled by Smith et al. (1989) is provided.

Table 1: Summary of the main parameters forming the ecological units on Herschel Island.

Name for ecological units by SMITH et al. (1989)	Ecological units (defined by Obu et al. 2015)	Mean slope [°]	Slope range [°]	Ecological features	Gully erosion	Soil types	Dominant vegetation communities	Summed geomorphological appearences	Mean active layer thickness [cm] (relating on survey by SMITH et al. 1989)
Avadlek	spits and beaches	1	0 - 1	spits and beaches, coastal and marine accumulation forms	marine erosion and deposition	Regosolic Static Cryosol	Wild Rye, Sandwort, Lungwort	rare ice wedge, wedge polygons	90
Guillemot	**wet polygonial terrain**	**2**	**0 - 3**	**depressional polygonal ground, frost cracking and peat accumulation**	**hardly**	**Gleysolic Turbic Cryosol**	**Cottongrass, Moss**	**low and high centre ice wedge polygons**	**23**
Herschel	**hummocky tussock tundra**	**1**	**0 - 4**	**Smooth uplands**	**hardly**	**Orthic Turbic Cryosol**	**Cottongrass, Moss**	**occasional vegetated circles by frost lift**	**20**
Komakuk	**slightly disturbed uplands**	**4**	**0 - 6**	**sloping uplands, slow downslope movemnets and gelifluction**	**slightly**	**Orthic Turbic Cryosol**	**Arctic Willow, Dryas-Vetch**	**earth hummocks, non-sorted nets and circles**	**30**
Orca	alluvial fans	2	1 - 5	alluvial fans and accumulation	depositional	Regosolic Static Cryosol	Sedge, Grass	occasional ice wedge polygons	45
Plover	**moderately disturbed terrain**	**5**	**2 - 14**	**active failing and moderate downslope movements, strongly gullying terrain and active-layer detachments**	**slightly**	**Regosolic Turbic Cryosol**	**Arctic Willow, Dryas-Vetch**	**extensive non-sorted nets and circles**	**40**
Jaeger	**moderately disturbed terrain**	**6**	**2 - 18**	**sloping, gullied terrain**	**moderately**	**Regosolic Static Cryosol**	**Willow, Saxifrage-Coltsfoot**	**earth hammocks, non-sorted nets and circles**	**46**
Thrasher	strongly disturbed terrain	15	12 - 27	active failing, strongly gullied terrain; active coastal erosion, slumping and other mass wasting	massive	Regosolic Static Cryosol	Arctic Willow, Lupine-Lousewort	disrupted earth hummocks	55

According to Smith et al. (1989) and Obu et al. (2015). Smith et al. (1989) classified eight different units for the ecological environment of Herschel Island summarized in the table above. Along the study sites of Fox Creek only units in bold letters appear.

3.7. Fox Creek Valley

The study focuses on Fox Creek, a small valley that predominately underlies thermos-erosional processes. It is located on the eastern part of Herschel Island. The valley runs from an elevation of 70 m.a.s.l. in the inland and extends over a distance of circa 1 300 m from the source to its outlet at the coastline to the Beaufort Sea (*map 1*).

The valley is characterized by the presence of a degrading polygon tundra net on the uplands and mainly develops by thermal erosion, which can be verified by gelifluction, active layer detachments and gullying on its gentle slopes. Down the valley mass wasting processes impact the slopes, which become steeper (*figure 4*). On the steeper slopes, in the lower part of the valley the stream incises the ground deeper, showing barren ground walls along the stream. The closer the valley gets to its outlet the more the valley symmetry changes, visible by more irregular slope surfaces. *Map 3* gives an overview on the changing slope gradients with advanced distance to the source. In Fox Creek, generally small tundra vegetation of shrubs, grasses, mosses and sedges forms the vegetative canopy. According to the degree of erosion, water content, soil sediments and remaining snowbanks during spring, the vegetative composition varies.

The ecological units that are present along the study site locations of the valley are *Herschel*, *Komakuk*, *Jaeger-Plover*, *Guillemot (map 2)*.Geomorphological units helped to locate separate the sites. ‘Uplands’ included all sites that were on the plateus, ‘bed’ summarized sites that were along the valley bottom close to the stream, and for ‘slopes’ samples locations were unified that appear between the scarp and the toe of a slope.

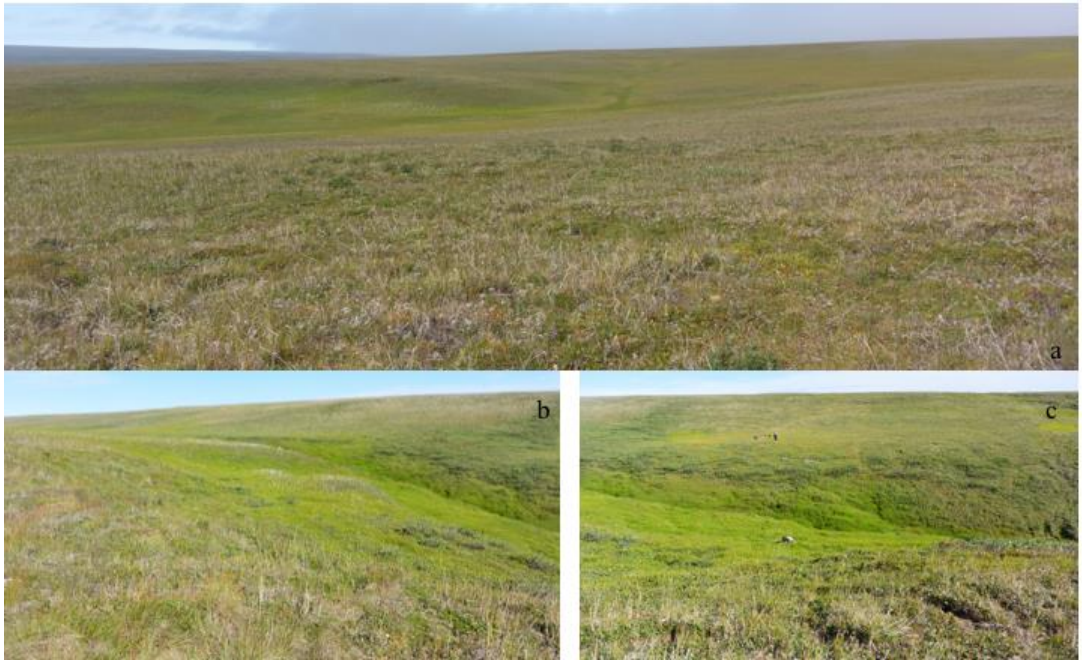

Figure 4: Overview on Fox Creek valley. Pictures were taken from different positions on the uplands. a) View on upper valley into source direction. Inside these area FC-T1 and FC-T2 were located. b-c) View from lower valley position (FC-T3) (Photo: J.Ramage, AWI).

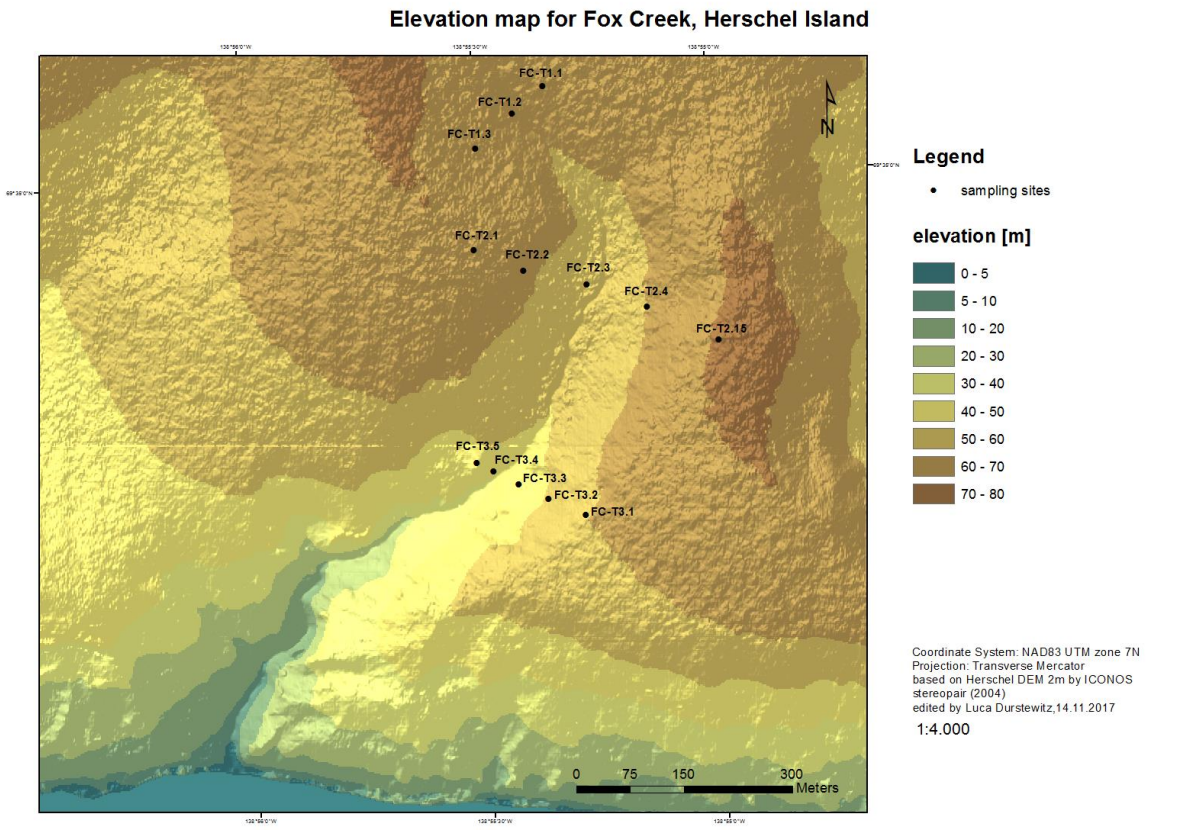

Map 1: Elevation map for Fox Creek, Herschel Island.

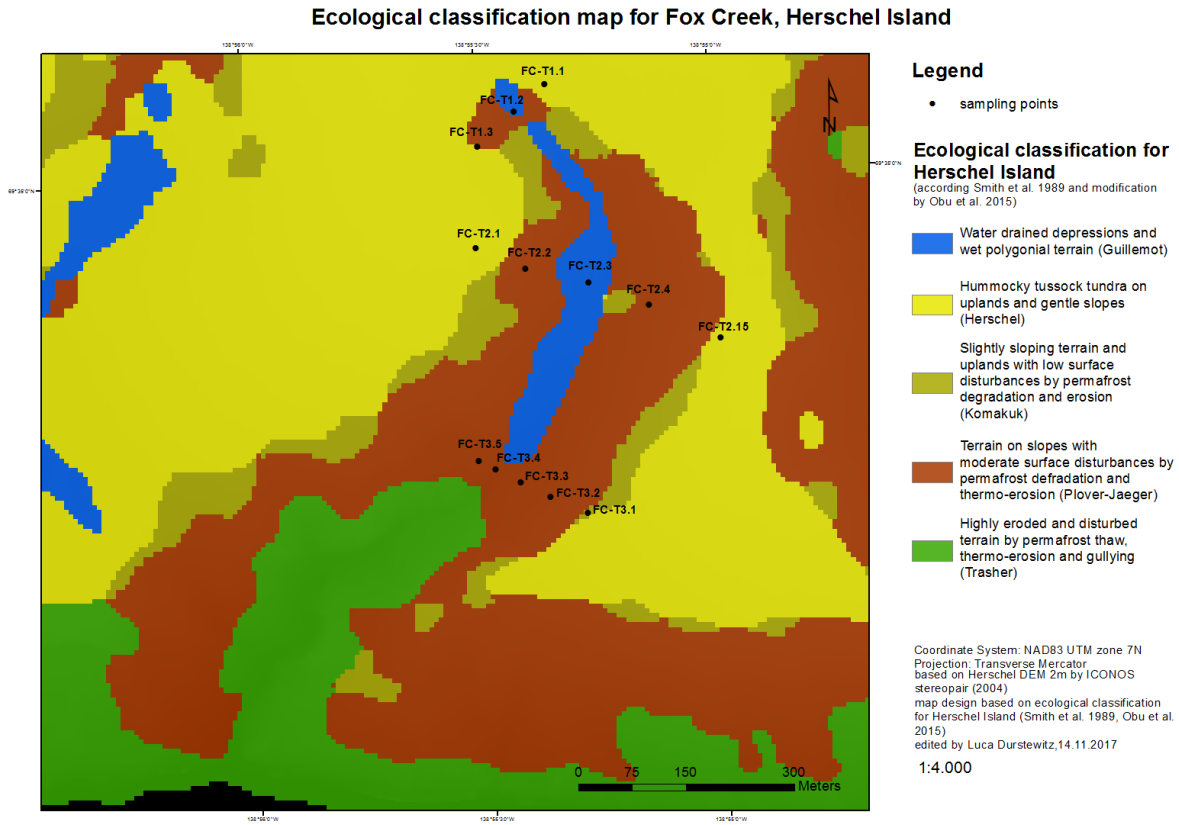

Map 2: Elevation map for Fox Creek, Herschel Island.

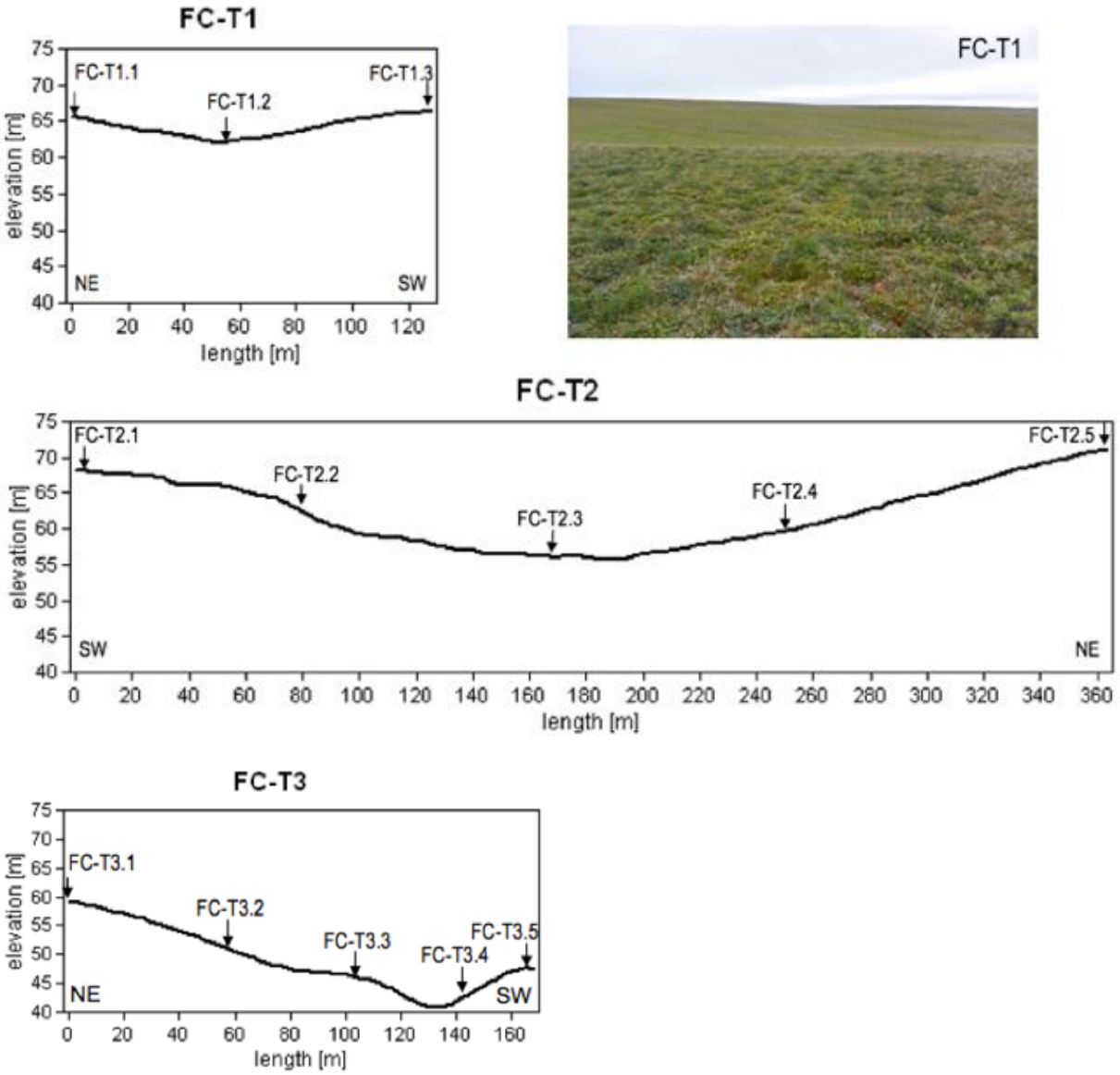

Figure 5: Transect profiles and site positions. With an overview picture on the location of the upstream transect (Photo: J.Ramage, AWI).

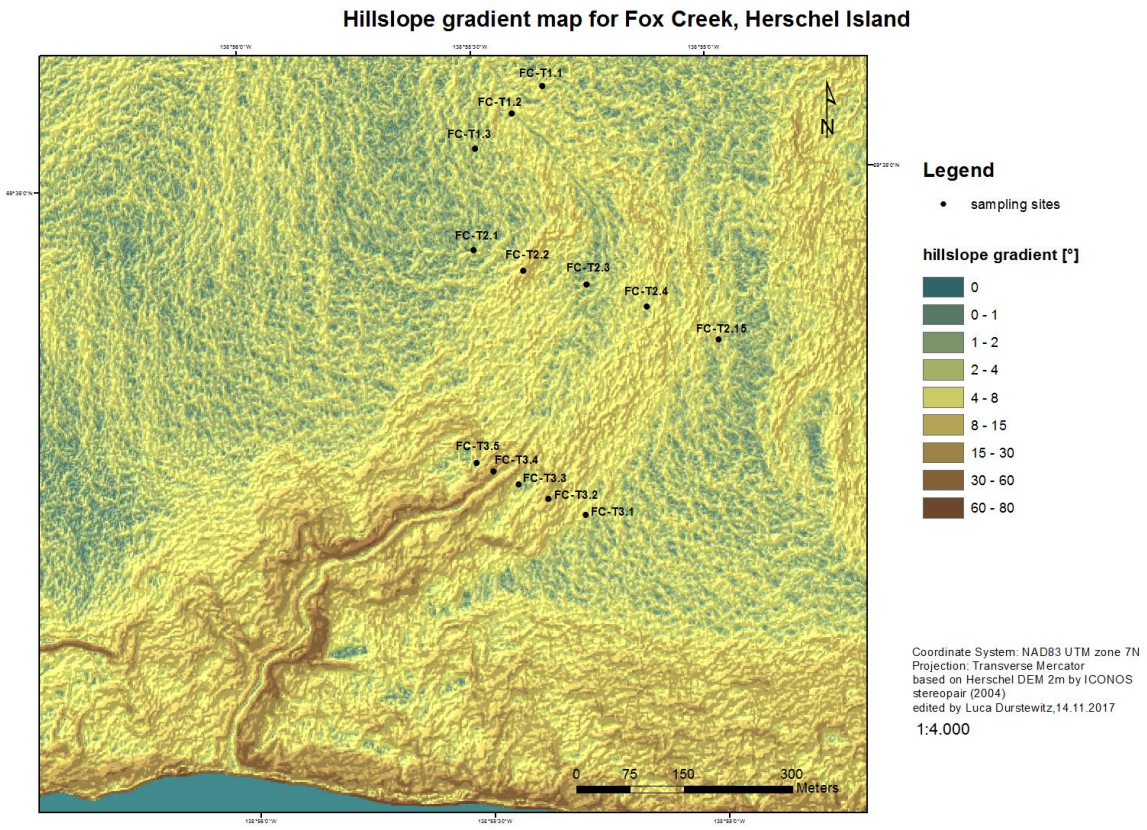

Map 2: Hillslope gradient map for Fox Creek, Herschel Island.

4. Methods

4.1. Field Work

In summer 2015 soil samples of 100 cm depth were taken along three transects across the valley to guarantee a transition trough different geomorphological features and ecological units. Along each transects, 3 to 5 sites were selected for coring (*figure 5*). The site crossed valley uplands, slopes and bed and were each site was localized with DGPS. By surrounding conditions every pit was grouped to its location on hillslope position, valley level and ecological unit. To examine the soil processes of each site pits were dug down to the permafrost table (*figure 6*). In the active layer, the samples were collected horizontally with the aid of fixed volume cylinders. A detailed survey of soil properties such as soil type, particle size, roots, buried organic matter occurrence were noted. In the permafrost, samples were extracted utilizing a steel pipe that was hammered manually into the ground for the remaining decimeters. Subsequently, all samples were weighted and stored cool until laboratory processing in Potsdam, Germany.

Figure 6: Soil sampling during field survey. a) Soil surface and vegetation cover on the upland at transect 1 (Herschel); Sampling pit on the upland in transect 1 (b), on a slope transect 3 (Plover-Jaeger) (c), in the bed (Guillemot)(d). (e-f) Core samples from permafrost ground (Photos: J.Ramage, AWI)

4.2. Laboratory Methods

As a preparation for further laboratory analysis, at first all individual samples (n = 93) got freeze dried for 72 hours and then dry weight was measured to calculate the water content and dry bulk density (BD). Afterwards every sample got divided for different laboratory analyses.

4.2.1. Dry Bulk Density

The dry bulk density is the weight of dry soil divided by the total soil volume (given in *equation 1*).

In order to estimate total nitrogen (TN) and total organic carbon (TOC) dry bulk density was needed to convert the weight-based value to its volume-based value (Strauss et al. 2015: S 1.3).

(1) $\rho_b = m_d / v_t$

ρ_b = *dry bulk density [g/cm³]*
m_d = *sample dry weight [g]*
v_t = *total volume [cm³]*

4.2.2. Elemental Analysis: Total Nitrogen, Total Carbon and Total Organic Carbon

To estimate the carbon and nitrogen elements in soil samples, all samples were first homogenized manually and then grinded with a mill during 6 minutes for organics and 8 minutes for minerals before being measured in a carbon-nitrogen-sulphur analyzer. For every subsample 5 g was weighted and transferred in zinc capsules for the measurement in the elemental analyzer (Vario EL III, Elementar). To ensure a total oxidation by high temperature combustion tungsten-(VI)-oxide (10 mg) was added to every subsample. This method brought the sample to high temperatures in order to get the elements mobilized into their gaseous phases, allowing a separation of the molecules by integrated absorption columns, and to detect them due to their thermal conductivity (Eischeid 2015: 26). Subsequently the TN and TC percentage could be estimated referring to the samples' input weight. During the measurement, blank samples were involved and processed equally for the detection of background noises (Strauss et al. 2015: S1.2).

$TOC_{wt\%}$ was calculated referring to the previous estimation of $TC_{\%}$ by the elemental analyzer. The TOC analyzer (Vario Max C, Elementar) was configured to lower temperatures so that only OC compounds was able to enter the gaseous phase (Eischeid 2015: 26). For that crucibles were prepared to measure its weight, up to 100 mg according to the $TC_{\%}$ content that was measured before. Also in this analyzing process blanks helped to reconstruct background signals.

4.3. Data Processing

4.3.1. Soil Properties

Since only one sample was taken in each horizon in the active layer, and every 10 cm in the permafrost soil, each sample was interpolated to a length of their horizon. Hereby a representative value of the SOC storage of a horizon can be evaluated (*equations 2 & 3*).

(2) $TOC = [\ \rho_b \times (\ TC_{wt\%} / 100\ ) \times h\ ] \times 10$

TOC = total organic carbon [kg/m²]
ρ_b = dry bulk density [g/cm³]
$TC_{wt\%}$ = total carbon [wt%]
h = height of sample horizon [cm]

(3) $TN = [\ \rho_b \times (\ TN_{wt\%} / 100\ ) \times h\ ] \times 10$

TN = total nitrogen [kg/m²]
ρ_b = dry bulk density [g/cm³]
$TN_{wt\%}$ = total nitrogen [wt%]
h = height of sample horizon [cm]

4.3.2. C/N Ratio

The TOC and TN relationship was visualized by using the C/N weight ratio. C/N is a reliable proxy for the reconstruction of soil properties by its organic matter decomposition degree within soils (Meyers 1997: 219). This assumption is based on a differing relation between C to N during the composition of organic matter substrates by microorganisms. Since the metabolic activity of microorganisms in aerated soil deposits preferentially mineralize carbon and immobilize TN so that nitrogen compounds get left behind (Palmtag et al. 2016: 480; Strauss et al. 2015: 2230). The more decomposition of organic substrates takes place, the lower the C/N ratio value falls. Generally, it can be stated that the ratio decreases at lower depth within a soil profile (Stevenson 1994: 100).

In this study, the C/N ratio was therefore used as a helpful hint for changes of decomposition along different geomorphological features within a TEV.

4.3.3. Statistical Analyses

According to the field observations, all sites were classified to a subgroup of each corresponding landscape classification (*table 2*) to allow statistical analyses.

To highlight the significant difference between all groups the means for the whole pit and of the active layer were tested by using the analysis of variances test (ANOVA). A statistical significant difference is detected when the $p < 0.05$. Anyway, the ANOVA requires a Gaussian distribution of the values within a group. Therefore, the normality of the distribution was tested by using a Shapiro-Wilk test on the dataset. This statistical pre-test for significance is useful for a small sample population ($n < 30$). The H_0 gets accepted when $p > 0.05$ which means that the values are distributed normally.

Moreover, correlation occurrences (Pearson) between the active layer depth and the TOC, TN and C/N values within the whole pit and within the active layer part, respectively, were tested.

All statistical analyses were calculated with the use of statistical software packages of R Studio (Appendix).

Table 2: Subdivision of sample sites in environmental units.

FC-T1	FC-T2	FC-T3	Upland	Slope	Bed	Herschel	Komakuk	Guillemot	Plover-Jaeger
FC-T1	FC-T2.1	FC-T3.1	FC-T1.1	FC-T2.2	FC-T1.2	FC-T1.1	FC-T2.5	FC-T1.2	FC-T2.2
FC-T2	FC-T2.2	FC-T3.2	FC-T1.3	FC-T2.4	FC-T2.3	FC-T1.3	FC-T3.5	FC-T2.3	FC-T2.4
FC-T3	FC-T2.3	FC-T3.3	FC-T2.1	FC-T3.3	FC-T3.2	FC-T2.1			FC-T3.2
	FC-T2.4	FC-T3.4	FC-T2.5	FC-T3.4		FC-T3.1			FC-T3.3
	FC-T2.5	FC-T3.5	FC-T3.1						FC-T3.4
			FC-T3.5						

4.3.4. Visualization

For every site one graph containing the storage of TOC and TN and the relating C/N ratio within the soil profile was plotted using the software Grapher 9.0 (*Appendix*). Due to missing data, the elemental soil properties FC-T3.2 could not be plotted.

To display the distribution of TOC, TN and C/N values of the total soil site along different groups within Fox Creek valley box-whisker plots were used as visualization. As a comparison of the distribution of these parameters, a set of box-whisker plots also got created for the active layer and permafrost part of the sites (*Appendix*).

The boxplots were created with the use of statistical software packages of R Studio (*Appendix*).

5. Results

5.1. Distribution of TOC and TN

5.1.1 Within the valley

In Fox Creek, the storage and distribution of TOC and TN differed (*table 3*). Some locations showed higher contents in soils than others. Depending on the terrain and position, an accumulation or loss of TOC and TN occurred.

Along the upper positions of a hillslope, the highest values for TOC and TN were observable (31.6 ± 6.3 kg/m²; 2.4 ± 0.5 kg/m²). Low values were found on the slopes, terrain that was moderately disturbed by downhill movements (18.4 ± 6.6 kg/m², 1.6 ± 0.4 kg/m²). Intermediate values occurred within accumulating areas at the foot of the slopes with an average of 27.0 ± 11.9 kg/m² and 2.0 ± 0.7 kg/m², respectively.

Regarding the ecological unit, the distribution of TOC and TN stocks differed as well. The distribution was similar to the observations made for hillslope positions. Along the ecological unit in slightly or low disturbed terrains, like *Herschel* (31.3 ± 6.7 kg/m²; 2.3 ± 0.5 kg/m²) and *Komakuk* (32.3 ± 5.6 kg/m²; 2.4 ± 0.3 kg/m²), high stocks of OC and nitrogen were detected.

The highest mean values were reached along the peaty wet terrains of the *Guillemot* unit (35.3 ± 2.5 kg/m²; 2.5 ± 0.3 kg/m²).

Table 3: Mean TOC, TN, C/N values and the mean active layer depth for each subgroup.

	mean TOC [kg/m²]	mean TN [kg/m²]	mean C/N	mean AL depth [cm]
FC-T1	31.2 ± 5.0	2.3 ± 0.4	13.6 ± 0.9	42.0 ± 5.0
FC-T2	30.0 ± 7.7	2.3 ± 0.5	13.1 ± 1.4	45.2 ± 5.9
FC-T3	20.2 ± 10.7	1.7 ± 0.6	11.4 ± 1.8	73.8 ± 18.9
Upland	31.6 ± 6.4	2.4 ± 0.5	13.4 ± 0.7	48.2 ± 5.3
Slope	18.4 ± 6.6	1.6 ± 0.4	11.2 ± 1.2	68.3 ± 20.5
Bed	27.0 ± 11.9	2.0 ± 0.7	12.8 ± 2.5	53.0 ± 23.4
Herschel	31.3 ± 6.7	2.3 ± 0.5	13.4 ± 0.8	47.5 ± 6.4
Komakuk	32.3 ± 5.6	2.4 ± 0.3	13.4 ± 0.4	49.5 ± 0.5
Guillemot	35.3 ± 2.5	2.5 ± 0.3	14.5 ± 0.9	36.5 ± 2.5
Plover-Jaeger	16.8 ± 6.7	1.5 ± 0.4	10.8 ± 1.3	71.8 ± 21.1

Averages are given with standard deviation.

With *Figure 7* the distribution of TOC and TN storage within the valley got visualized. Statistical analysis showed that all subgroups had a normal distribution, but for the spread of TOC and TN no significant differences were detected. This missing statistical validation could be explained by a small sample population within the subgroups of *Komakuk* (n = 2) and *Guillemot* (n = 2).

The boxplots helped to reconstruct the spatial distribution of carbon and nitrogen stocks in the valley, even though they could not demonstrate a clear statistical division along the subgroups of ecological unit, hillslope positions units and transect location was not given.

High OC stocks were found along the uplands and in the valley bed. The variances inside the classes were relatively high (*figure 7*). Also along the upstream transect, where smooth slopes were dominant, the TOC and TN contents were higher. With increasing distance to the source the values decreased.

According to the ecological unit, the boxplots show that high carbon and nitrogen stocks were distributed along the *Guillemot* unit, followed by the *Komakuk* unit and *Herschel* unit. Between these values of TOC and TN storage and the ones of the *Plover-Jaeger* unit, representing sloping terrain, the values decreased strongly.

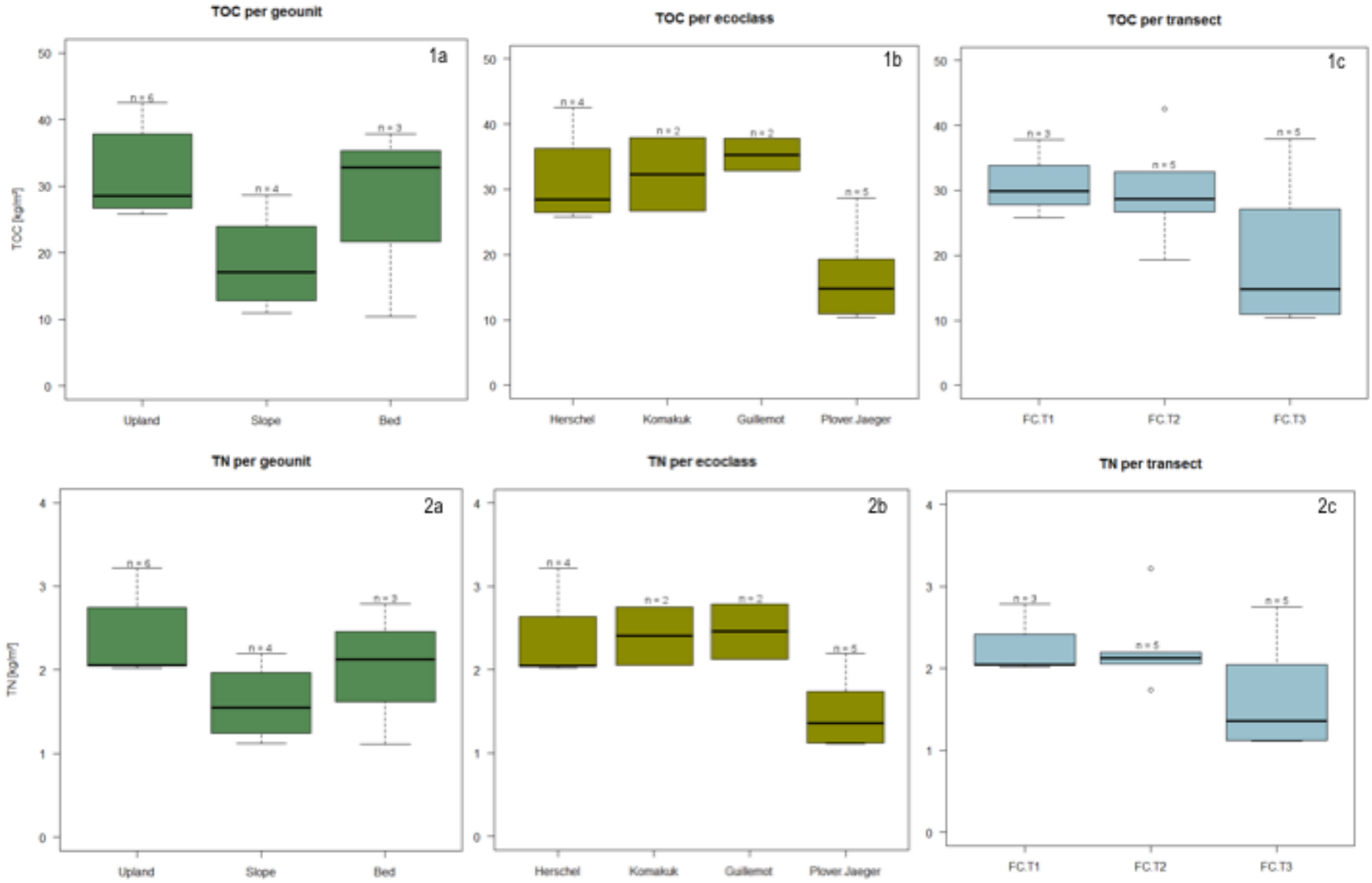

Figure 7: Boxplot for TOC and TN distribution within the valley. Comparison of TOC (1a-c) and TN stocks (2a-c) (kg/m^2) within valley soils (0-100 cm) depth between valley position, ecological unit and transect. a: geomorphological unit (Upland, Slope, Bed); b: ecological units (*Herschel*, *Komakuk*, *Guillemot*, *Plover-Jaeg*er); c: valley level, transects (FC-T1, FC-T2, FC-T3)

5.1.2. Between active layer and permafrost

TOC and TN contents differed also vertically in each site. By examining the soil samples of every site it was shown that stocks generally changed between the active layer and the permafrost layer. TOC and TN values were mostly higher in the seasonally thawed layer than in the permafrost soil (*Appendix*).

Within the valley, the active layer depth along sites varied and different amounts of TOC and TN were observed within the active layer (*table 3*). Statistical analyses showed that TOC and TN values of an entire pit correlated negatively with the depth of active layer (r^2 = -0.81; r^2 = -0.74) (*table 4*). Moreover, there was a low negative correlation between the TOC values of the active layer and its depth (r^2 = -0.57).

Generally, a decrease of TOC and TN from the upper most part of the active layer down to the permafrost table was oberservable. The values proceed only by a moderate decline. Some pits showed a different vertically trend mostly in relation to their hillslope position. Samples extracted on slopes showed no continuety of TOC and TN contents along the soil profiles. TOC and TN values were remarkably low in permafrost (< 5 $TOC_{wt\%}$; < 0.5 $TN_{wt\%}$). At two sites (FC-T2.2, FC-T2.4) the profiles displayed a strong decrease of TOC and TN in the active layer but low and smoothly ranging values in permafrost. Whereas at other sites (FC-T3.3, FC-T3.4) the decrase of TOC and TN in the active layer was lower and showed even more shallow values in the permafrost layer.

For a detailed survey on every pit trend profiles are given in a table and as boxplots in the Appendix.

Table 4: Pearson correlation values between TOC, TN, C/N.

Pearson	Total pit			Active layer		
r^2	TOC	TN	C/N	TOC	TN	C/N
Active layer depth	-0.81	-0.74	-0.89	-0.57	-0.34	-0.75

Correlation between TOC, TN and C/N values of the total pit (and active layer) with active layer depth.

5.2. Distribution of C/N

5.2.1. Within the valley

The C/N ratio showed spatial differences in decomposition of organic matter in the valley (*figure 8*). C/N values of a whole pit had a relative strong correlation with the active layer depth (r^2 = - 0.89). The strong correlation also existed between the C/N values of the active layer and the active layer depth (r^2 = - 0.75).

A relationship between the spread of high C/N values and the spread of high TOC and TN contents was recognizable within the valley. A statistically clear defined separation of the groups (ecological unit, geomorphological units, transects) were missing mostly, though, due to the sample population ($n \leq 6$) Only between two ecological unit, *Herschel* and *Plover-Jaeger*, a statistical significant difference ($p = 0.0136$) was detected.

The spatial availability according to the ecological units displayed the lowest ratios in attributed *Plover-Jaeger* sites belonging to zones on slopes where surface soil was exposited and subjected to erosion. For the *Herschel* and *Komakuk* unit which were situated in hummocky terrains and along gentle slopes the C/N values were higher, followed closely by the highest C/N values that were localized in the *Guillemot* area where water lodging and peat accumulation were usual (*table 3*).

Additionally, high values of C/N in Fox Creek were displayed along soils of the upslope positions. Slightly higher ratios were observable along the valley bed (12.8 ± 2.5).

Within the valley the carbon availability changed according to the level position. Upstream positions, crossing gentle slopes with slightly eroded surfaces, showed a C/N ratio distribution that revealed lower decomposition rates. Low C/N ratios and therefore a high decomposition were found along the lower transect FC-T3 (11.4 ± 1.8), which was positioned on the downstream, closest to the outlet where hillslopes started to become steeper.

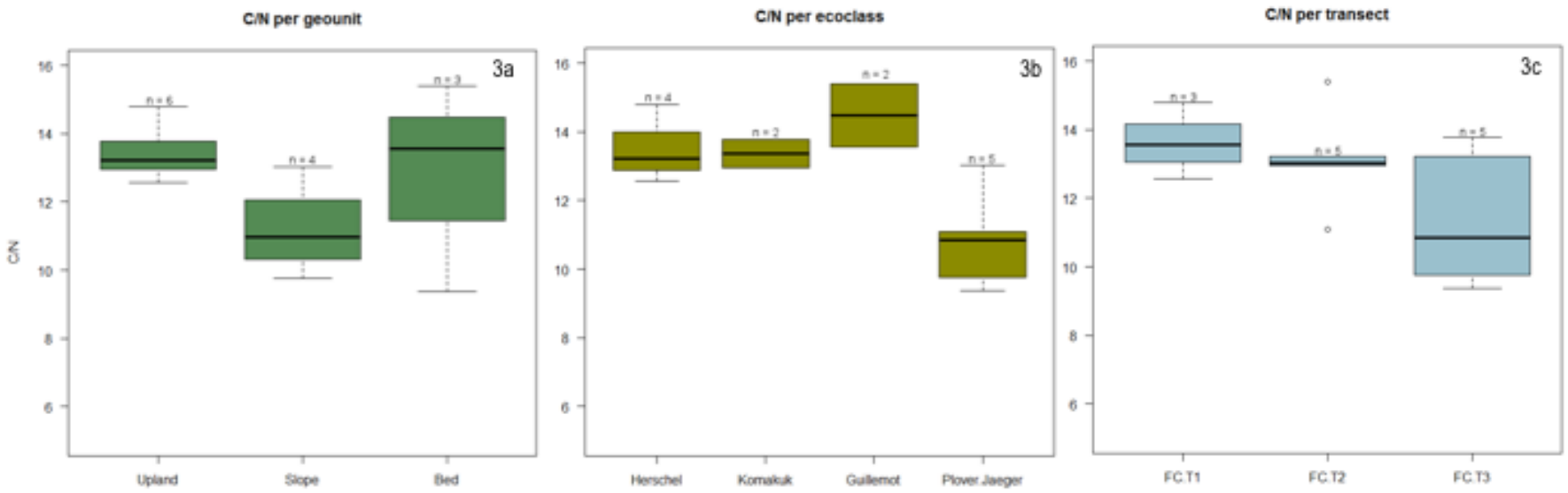

Figure 8: Boxplots for C/N distribution within the valley. Comparison of C/N Ratio within valley soils (0-100 cm) between geomorphological unit (3a), ecological unit (3b) and transect (3c). Significant differences occur between Herschel and *Plover-Jaeger* ($p = 0.0136$).

5.2.2. Between active layer and permafrost

C/N ratios vary vertically in the soil sites. Main differences arise between the active layer and permafrost. In the active layer, higher values were also observable and correlated with its depth (r^2 = - 0.75). Near the surface the values were highest and decreased until the permafrost table. Within the permafrost table the C/N values fell with increasing depth. In total, the ratio decreased from the uppermost part of the soil profile (active layer) from nearly 40 to a value below 10 (permafrost at 100 cm depth). Only at site FC-T3.1 an increase of C/N in the permafrost took place. Some leaps of the C/N values were observed within the permafrost ground. These outlying values normally appeared together with leaps of TOC and TN content.

It could be observed that the C/N ratio changed at depth when TN values exceeded in comparison to values of TOC.

For a detailed visualization of the C/N ratio trend for each site see Appendix.

6. Discussion

The main aim of this thesis was to determine the general spatial distribution of TOC, TN and C/N within an arctic valley, shaped by thermo-erosional processes. The underlying hypothesis predicted that spatial patterns of SOC and TN stocks buried in soils are driven by geomorphological processes. The focus of this study was on the analysis of the horizontal and vertical spatial variability of storage and decomposition characteristics in soils within Fox Creek valley on Herschel Island.

Previous studies (Hugelius et al. 2012; Pizano et al. 2014; Palmtag et al. 2015; Obu et al. 2015; Siewert et al. 2016; Shelef et al. 2017) assumed that in areas of continuous permafrost, storage rates differed at the local scale due to topography and geomorphological processes.

In this study, spatial differences in storages and decomposition rates related to their positions were also detected within Fox Creek valley.

The highest values of TOC and TN were found on the uplands, characterized by plain or smoothly sloping terrains. At these locations, the soils were usually characterized by a thin active layer and dense vegetation cover which were regulating factors for the thermal and hydrological conditions of the soil and protected subjacent permafrost from seasonal thaw (Siewert 2016: 15, Pizano et al. 2014: 2). The decomposition was slow (high C/N), microbial activity was limited in the shallow upper soil parts and prohibited in lower soil horizons due

to the frozen state (Harms et al. 2014: 300, Hugelius et al. 2014: 6574). The negative correlation between TOC and TN values and the active layer depth confirmed this phenomenon: the greater the active layer depth, the less the carbon and nitrogen storage.
Values of TOC and TN in areas along the valley bed were slightly lower even though anoxic conditions obtain these soils. Along these sites accumulation of colluvial and alluvial deposits was more likely than erosion and surface disturbances. The mobilized material got concentrated here, which led to high amounts of TOC and TN storage (Shelef et al. 2017: 2, Young 1972: 62).
Along the upland and valley bed areas, fresh *in situ* accumulation of carbon was usual, driven by vegetation growth during the summer season. Hence, soils are enriched in TOC and TN (Hobbie et al. 2000: 198).

The ecological units characterizing uplands (*Herschel* and *Komakuk*) had higher TOC and TN contents (*table 3*) and the decomposition rates averaged all at 13.4 ± 0.4 (-0.8). *Komakuk* featured slightly higher values for TOC and TN stocks than *Herschel*, though. This aspect was actually contrary to the hypothesis that slope angle was associated with greater degradation and hence with smaller C/N ratios.
The *Komakuk* zone is characterized by gently sloping terrain with angles of 4° and is subjected to gelifluction and a deeper mean active layer (49.5 ± 0.5 cm). These factors should facilitate decomposition rates due to stronger aeration of surface soils since water runs off more easily (Hobbie et al. 2000: 202). The higher values observed here could be attributed to local soil characteristics (Hugelius et al. 2014: 6574), vegetation cover and types or microbial organisms (Hobbie et al. 2004: 340; Siewert 2016: 15, Palmtag 2016: 489). Within the *Komakuk* unit, arctic willow (*Salix arctica*) was the dominant vegetation species that may influence the higher TOC stocks due to its residues. Woody stems probably slowed down the decomposition by soil microorganisms (Hobbie et al. 2000: 197; Weintraub & Schimel 2003: 130). But also, incorporation of TOC and TN in deeper horizons by cryoturbation could likewise led to increased stocks (Siewert et al. 2016: 16). Nonetheless, the values reported here for *Komakuk* should be taken with caution, since the unit only comprised two sites. Siewert (2016: 11), instead, analyzed 12 sites attributed to *Komakuk* in a neighboring location and showed that the *Komakuk* zone was characterized by lower SOC storage than the *Herschel* zone. This numbers would confirm the fact that TOC lability is linked to slope gradient and its enhanced downslope movements.

The *Guillemot* unit had high values of TOC (35.3 ± 2.5 kg/m^2) and C/N (14.5 ± 0.9) contradictorily to those of the valley bed (27.0 ± 11.9 kg/m^2; 12.8 ± 2.5). *Guillemot* samples were located close to the stream were the soils were water-saturated. Due to the lack of oxygen microbial decay processes got decelerated (Davidson & Janssen 2006: 165; Hobbie et al. 2000: 198). Thus, carbon and nitrogen stocks increased by hindered decomposition and by deposited material of hillslope processes (Pizano et al. 2014: 9, Shelef et al. 2017: 1). Hence, the TOC content and C/N ratio rose (Hobbie et al. 2000: 198). However, also Guillemot had a small sample population (n = 2).
Even though, slightly differences appeared along the units of undisturbed surface terrain, the TOC and TN stocks and the C/N ratio were high.

On slopes, the values for TOC, TN and C/N were the lowest. Hillslopes with a mean gradient of 5-6° were more disturbed by moderate mass movements, active layer detachments or gullying processes (*map 3*). The stocks on slopes were similar to those of the *Plover-Jaeger* unit (which covers roughly the same area), thus both subgroups will be discussed together.
Due to surface disturbances the biological and physical processes got altered, which impacted the availability of OC (Pizano et al. 2014: 2). Enhanced material loss, deeper active layers and higher water drainage due to slope angle allowed aeration of lower soil horizons and facilitated remineralization processes (Hobbie et al.: 2000: 202). The availability of OC for decomposition along these valley positions was higher because previously cryoturbated and isolated organic matter pockets became available again for microbial activity (Palmtag et al. 2016: 491). This led to a strong decrease in carbon stocks and C/N ratio. These storage and availability differences between terrains of disturbed and undisturbed surfaces could be once detected as statistically significant, between *Herschel* and *Plover-Jaeger*.
On sloping terrain with unconsolidated sediments in cold climates slow mass wasting can initiate by a slope gradient of 1° (Washburn 1973: 73-75). Fine, silty sediments are able to hold more water and were therefore likely to exceed local stability thresholds (Washburn 1973: 175). As a result, movements down the slopes occurred due to volume loss and ground destabilization by ice melt (Pizano et al. 2014: 2). Melted ice additionally increased thermo-erosional processes on slopes that enhanced gullying events and triggered material mobilization towards the hill toes and the stream (Shelef et al. 2017: 2; Lamoureux et al. 2014: 5502, Poesen et al. 2003: 101). Thermo-erosion liberated deeper soil parts to further thaw, thereby increased the availability of previously buried carbon (Hugelius et al. 2014: 6589; Pizano et al. 2014: 2; Obu et al. 2015: 102). Due to these processes, TOC, TN and C/N

values decreased on slopes (Shelef et al. 2017: 1; Harms et al. 2014: 308, Hugelius et al. 2014: 6589; Poesen et al. 2003: 99).

Distributive differences of TOC, TN and C/N stocks also occurred along the transect locations in the valley.

In the upper (FC-T1) and middle parts of the valley (FC-T2), higher values for TOC, TN and C/N were measured in comparison to the lower part (FC-T3). These could be explained by generally lower active layer depths in the upper transects (42.0 ± 5.0 cm; 45.2 ± 5.9 cm) than in the lower transects (73.8 ± 18.9 cm).

In addition, the morphology of hillslopes and its characterizing dominant erosional processes should be also taken into account when comparing TOC and TN storage along transects and their storage rates of TOC and TN. Yoo et al. (2006) started a survey campaign on SOC distributions and availability within two Californian valleys. They saw that local conditions (i.e. topography, plant input, decomposition, soil texture, nutrients and moisture) were highly likely to influence the variation of SOC storage in the valleys. Even though climate conditions, weathering, soil taxa and ecology are highly different to those in the Arctic, links to slope forms and erosive processes are possible. Yoo et al. (2006) recognized that SOC storages varied with slope curvature. They noticed that if convergent slopes increased in concavity, higher SOC stocks occurred (Yoo et al. 2006: 54). These storage rates in turn could be linked to the dominating erosional process controls (Yoo et al. 2006: 55).

For Fox Creek, similar observations were made. In valleys that were accentuated by thermo-erosion, the hillslope concavity decreases from the upstream to the downstream (*figure 5*) (Parsons 1988: 90). Through time, hillslope on unconsolidated deposits reduce their gradients leading to lower slope angles, rounded crests and colluvial foot slopes (Parsons 1988: 90). Material on concave hillslopes got mobilized and accumulated toward the valley bed by slow operating creeps and fluvial processes (Parsons 1988:90; Shelef et al. 2017: 7). Erosions along the upstream transects were low and thus considerable amounts of TOC and TN get stored (Shelef et al. 2017: 8).

At the lower valley level, the slopes got steeper, concavity decreased and the incision by the stream was greater. According to Yoo et al. (2006), those slopes had a higher loss of TOC and TN. This was also detected in Fox Creek. Surface disturbances were common and thermo-erosional processes occurred more easily that led to a rise in exportation of already decomposed soil material by fluvial outwash (Lamoureux & Lafrenière 2014: 8). Low values of TOC and TN stocks probably intensified during snow melt periods when the exportation

rate of labile material was stronger since vegetation just started recovery and meltwater run off in gullies enhanced (Godin et al. 2014: 7; Lamoureux et al. 2014: 5501).

Furthermore, the decomposition rates are higher (low C/N) along the lower transect due to deeper active layers and surface irregularities. The presence of small depressions along the lower transect probably permitted snow banks to endure late into summer months. Underneath the snow cover, microscale thermo-erosion manipulated the heat conductivity conditions, also during winter, and generated a longer period where surface soil was vulnerable to decomposition (Harms et al. 2014: 300; Tanski et al. 2017: 443).

7. Conclusion & Outlook

This study was able to point out that not only soil processes differed locally and influenced the carbon availability but that also local geomorphology and erosion processes had a strong influence.

The availability of carbon was linked to local hillslope positions, ecological conditions, soil processes and valley location. Local terrain factors influenced the carbon storage: low stocks were found along the slopes that were affected by erosional processes. High carbon stocks were localized on uplands and in the valley bed.

This spatial distribution applied to the variability of C/N ratio within the valley. On the uplands and in the bed, C/N ratios were high; on slopes the C/N ratio was low.

The main driving factors for carbon storage, decomposition (and therefore its availability) were active layer depth, hillslope gradient, hillslope processes and biological activity. All these factors change the hydrological and thermal conditions and increase the bioavailability of OC. Generally, it can be said that the more eroded a terrain the lower the carbon storage ability.

In summary, this study provides an overview on the distribution of organic matter in a single valley underlain by permafrost. In order to reduce the uncertainty of carbon stock variability and its availability, it would be necessary to investigate this spatial distribution in several valleys at local and regional scales across the Arctic. Since continuous erosion and permafrost degradation may further impact high-latitude landscapes, getting an overall picture of the carbon availability of permafrost soils across the Arctic would be an important goal for further research.

References

Barry, R.G. (1993): Canada's Cold Seas. In: French, H.M. & O. Slaymaker (Ed.): Canada's cold environments. Montreal, pp. 29-61.

Barry R.G. & T.Y. Gan (2011): The global cryosphere: Past, present and future. Cambridge, pp. 472.

Burn, C.R. & Y. Zhang (2009): Permafrost and climate change at Herschel Island (Qikiqtaruq), Yukon Territory, Canada. *Journal of Geophysical Research* 114, pp. 1-16.

Burn, C.R. (Ed.) (2012): Herschel Island: a natural and cultural history of Yukon's arctic island, Qikiqtaryuk. Calgary, pp. 242.

Davidson E.A. & Janssens, I.A. (2006): Temperature sensitivity of soil carbon decomposition and feedbacks to climate change. *Nature* 440, pp. 165-173.

Ehlers, J. & P.L. Gibbard (2007): The extent and chronology of Cenozoic Global Glaciation. *Quaternary International* 164 – 165, pp. 6-20.

Ehlers, J. (2011): Das Eiszeitalter. Heidelberg, pp. 363.

Eischeid, I. (2015): Mapping of soil organic carbon and nitrogen in two small adjacent Arctic watersheds on Herschel Island, Yukon Territory. Master thesis. University of Hohenheim, pp. 74.

French, H.M. (2007): The periglacial environment. 3rd ed., Chichester, pp. 458.

Friesen, M. (2012): Inuvialuit Archeology. In: Burn, C.R. (Ed.) (2012): Herschel Island: A natural and cultural history of Yukon's arctic island, Qikiqtaryuk. Calgary, pp. 146-152.

Fritz, M.; Wetterich, S.; Meyer, H.; Schirrmeister, L.; Lantuit, H. & W.H. Pollard (2011): Origin and characteristics of massive ground ice on Herschel Island (Western Canadian

Arctic) as revealed by stable water Isotope and hydrochemical signatures. *Permafrost and Periglacial Processes* 22, pp. 26-38.

Godin, E.; Fortier, D. & S. Coulombe (2014): Effects of thermo-erosion gullying on hydrologic flow networks, discharge and soil loss. *Environmental Research Letters* 9, pp. 1-10.

Graham D.E.; Wallenstein, M.D.; Vishnivetskaya, T.A.; Waldrop, M.P.; Phelps, T.J.; Pfiffner, S.M.; Onstott, T.C.; Whyte, L.G.; Rivkina, E.M; Gilichinsky, D.A.; Elias, D.A.; Mackelprang, R.; Verberkmoes, N.C.; Hettich, R.L.; Wagner, D.; Wullschleger, S.D. & J.K. Jansson (2012): Microbes in thawing permafrost: the unknown variable in the climate change equation. *International Society for Microbial Ecology* 6, pp. 709-712.

Günther, F.; Overduin, P.P.; Sandakov, A.V.; Grosse, G. & M.N. Grigoriev (2012): Thermo-erosion along the Yedoma Coast of the Buor Khaya Peninsula, Laptev Sea, East Siberia. In: Proceedings of the Tenth International Conference on Permafrost, Salekhard, Yamal-Nenets Autonomous District, Russia, June 25–29, edited by: Hinkel, K. M., vol. 1, International Contributions, pp. 137-142.

Günther, F.; Overduin, P.P.; Sandakov, A.V.; Grosse, G. & M.N. Grigoriev (2013): Short- and long-term thermo-erosion of ice-rich permafrost coasts in the Laptev Sea region. *Biogeosciences* 10, pp. 4297-4318.

Harms, T.K.; Abbott, B.W. & J.B. Jones (2014): Thermo-erosion gullies increase nitrogen available for hydrologic export. *Biogeochemistry* 117, pp. 299-311.

Hobbie, S.E.; Schimel, J.P.; Trumbore, S.E. & J.R. Randersons (2000): Controls over carbon storage and turnover in high-latitude soils. *Global Change Biology* 6(1), pp. 196-210.

Hugelius, G. (2011): Quantity and quality of soil organic matter in permafrost terrain. PhD thesis, Stockholm University, pp. 154.

Hugelius, G.; Routh, J.; Kuhry, P. & P. Crill (2012): Mapping the degree of decomposition and thaw remobilization potential of soil organic matter in discontinuous permafrost terrain. *Journal of Geophysical Research* 117, pp. 1-14.

Hugelius, G.; Strauss, J.; Zubrzycki, S.; Harden, J.W.; Schuur, E.A.G.; Ping, C.-L.; Schirrmeister, L.; Grosse, G.; Michaelson, G.J.; Koven, C.D.; O'Donnell, J.A.; Elberling, B.; Mishra, U.; Camill, P.; Yu, Z.; Palmtag, J. & P. Kuhry (2014): Estimated stocks of circumpolar permafrost carbon with quantifies uncertainty ranges and identified data gaps. *Biogeosciences* 11, pp. 6573-6593.

Jansson, S.L. & J. Persson (1982): Mineralization and Immobilization of Soil Nitrogen. In: Stevenson, F.J. (Ed.): Nitrogen in agricultural soils. Madison, pp. 229-252.

Jorgenson M.T. & J. Brown (2005): Classification of the Alaskan Beaufort Sea Coast estimation of carbon and sediment inputs from coastal erosion. *Geo-Marine Letters* 25, pp. 69-80.

Kennedy, M. (2012): Vegetation. In: Burn, C.R. (Ed.) (2012): Herschel Island: A natural and cultural history of Yukon's arctic island, Qikiqtaryuk. Calgary, pp. 80-86.

Kokelj, S.V.; Smith, C.A.S. & C.R. Burn (2002): Physical and chemical characteristics of the active layer and permafrost, Herschel Island, Western Arctic Coast, Canada. *Permafrost and Periglacial Processes* 13, pp. 171-185.

Lamoureux, S.F. & M.J. Lafrenière (2014): Seasonal fluxes and age of particulate organic carbon exported from Arctic catchements impacted by localized permafrost slope disturbances. *Environmental Research Letters* 9, pp. 1-10.

Lamoureux, S.F.; Lafrenière, M.J. & E.A. Favaro (2014): Erosion dynamics following localized permafrost slope disturbances. *Geophysical Research Letters* 41, pp. 5499-5505.

Lantuit, H. & W.H. Pollard (2005): Temporal stereophotogrammetric analysis of retrogressive thaw slumps on Herschel Island, Yukon Territory. *Natural Hazards and Earth System Science* 5, pp. 413-423.

Lantuit, H. & W.H. Pollard (2008): Fifty years of coastal erosion and retrogressive thaw slump activity on Herschel Island, southern Beaufort Sea, Yukon Territory, Canada. *Geomorphology* 95, pp. 84-102.

Lantuit H.; Overduin, P.P.; Couture, N.; Wetterich, S.; Aré, F.; Atkinson, D.; Brown, J.; Cherkashov, G.; Drozdov, D.; Forbes, D.L.; Graves-Gaylord, A.; Grigoriev, M.; Hubberten, H.W.; Jordan, J.; Jorgenson, T.; Strand Ødegård, R.; Ogorodov, S.; Pollard, W.H.; Rachold, V.; Sedenko, S.; Solomon, S.; Steenhuisen, F.; Streletskaya, I. & A. Vasiliev (2012): The arctic coastal dynamics database: a new classification scheme and statistics on arctic permafrost coastlines. *Estuaries and Coasts* 35, pp. 383-400.

Lenz, J.; Fritz, M.; Schirrmeister, L.; Lantuit, H.; Wooller, M. J.; Pollard, W.H.; Wetterich, S. (2013): Periglacial landscape dynamics in the western Canadian Arctic: Results from a thermokarst lake record on a push moraine (Herschel Island, Yukon Territory). *Paleogeography, Paleoclimatology, Paleoecology* 381-382, pp. 15-25.

Lewellen, R.T. (1970): Permafrost erosion along the Beaufort Sea coast. University of Denver, pp. 50.

Mackay, J.R. (1959): Glacier ice-thrust features of the Yukon Coast. *Geographical Bulletin* 13, pp. 5-21.

McGuire, A.D.; Anderson L. G.; Christensen, T.R.; Dallimore, S.; Guo, L.; Hayes, D.J.; Heimann, J.; Lorenson, T.D.; Macdonald, R.W. & N. Roulet (2009): Sensitivity of the carbon cycle in the Arctic to climate change. *Ecological Monographs* 79, pp. 523-555.

Meyers, P.A. (1997): Organic geochemical proxies of paleoceanographic, paleolimnologic and paleoclimatic processes. *Organic Geochemistry* 27, pp. 213-250.

Meyers, P.A. & J.L. Teraines (2001): Sediment Organic Matter. In: Last, W.M. & J.P. Smol (eds.): Tracking Environmental Changes Using Lake Sediments. Volume 2: Physical and Geochemical Methods. Dodrecht, pp. 239-269.

Morgenstern, A. (2012), Thermokarst and thermal erosion: Degradation of Siberian ice-rich permafrost. PhD thesis, University of Potsdam, pp. 116.

Myers-Smith, I.H.; Hik, D.S.; Kennedy, C.; Cooley, D.; Jonstone, J.F.; Kenney, A.J. & C.J. Krebs (2011): Expansion of canopy-forming willows over the twentieth century on Herschel Island, Yukon Territory, Canada. *AMBIO: A Journal of the Human Environment* 40 (6), pp. 610-623.

Obu, J.; Lantuit, H.; Myers-Smith, I.; Heim, B.; Wolter, J. & M. Fritz (2017): Effect of terrain characteristics on soil organic carbon and total nitrogen stocks in soils of Herschel Island, Western Canadian Arctic. *Permafrost and Periglacial Processes* 28, pp. 92-107.

Palmtag, J.; Hugelius, G.; Lashchinckiy, N.; Tamstorf, M.P.; Richter, A.; Elberling, B. & P. Kuhry (2015): Storage, landscape distribution and burial history of soil organic matter in contrasting areas of continuous permafrost. *Arctic, Antarctic and Alpine Research* 47 (1), pp. 71-88.

Palmtag, J.; Ramage, J.; Hugelius, G.; Gentsch, N.; Lashchinskiy, N.; Richter, A. & P. Kuhry (2016): Controls on the storage of organic carbon in permafrost soil in northern Siberia. *European Journal of Soil Science* 67, pp. 478-491.

Parsons, A.J. (1988): Hillslope form. London, New York, pp. 212.

Pizano, C.; Barón, A.F.; Schuur, E.A.G.; Crummer, K.G. & M.C. Mack (2014): Effects of thermo-erosional disturbance on surface soil carbon and nitrogen dynamics in upland acrtic tundra. *Environmental Research Letters*, pp. 1-13.

Poesen, J.; Nachtergaele, J.; Verstraeten, G. & C. Valentin (2003): Gully erosion and environment change: importance and research needs. *Catena* 50, pp. 91-133.

Pollard, W.H.; Couture, N. & H. Lantuit (2012): Coastal Environment. In: Burn, C.R. (Ed.) (2012): Herschel Island: A natural and cultural history of Yukon's arctic island, Qikiqtaryuk. Calgary, pp. 72-79.

Schaefer, K.; Lantuit, H.; Romanovsky, V.E.; Schuur, E.A.G. & R. Witt (2014): The impact of the permafrost carbon feedback on global climate. *Environmental Research Letters* 9, pp. 1-9.

Schuur, E.A.G.; Bockheim, J.; Canadell, J.G.; Euskirchen, E.; Field, C. B.; Goryachkin, S. V.; Hagemann, S.; Kuhry, P.; Lafleur, P. M.; Lee, H.; Mazhitova, G.; Nelson, F.E.; Rinke, A.; Romanovsky, V.E.; Shiklomanov, N.; Tarnocai, C.; Venevsky, S.; Vogel, J.G. & S.A. Zimov (2008): Vulnerability of permafrost carbon to climate change: implications for the global carbon cycle. *BioScience* 58 (8), pp. 701–714.

Shelef, E.; Rowland, J.C.; Wilson, C.J.; Hilley, G.E; Mishra, U.; Altmann, G.L.; Ping, C.-L. (2017): Large uncertainty in permafrost carbon stocks due to hillslope soil deposits. *Geophysical Research Letters* 44, pp. 1-11.

Siewert, M.B.; Lantuit, H. & G. Hugelius: Spatial variability of soil organic carbon in tundra terrain at local scale (in prep.) In: Siewert, M. B. (2016): High-resolution mapping and spatial variability of soil organic carbon storage in permafrost environments. PhD thesis, Stockholm University, pp. 54.

Smith, C.A.S.; Kennedy, C.; Hargrave, A.E. & K.M. McKenna (1989): Soil and vegetation of Herschel Island, Yukon Territory. Yukon Soil Survey Report No. 1. Land Research Centre, Agriculture Canada, Ottawa, pp. 101.

Stevenson, F.J. (1994): Humus chemistry: Genesis, composition, reactions. New York, pp. 512.

Strauss, J.; Schirrmeister, L.; Mangelsdorf, K.; Eichhorn, L.; Wetterich, S. & U. Herzschuh (2015): Organic-matter quality of deep permafrost carbon - a study from Arctic Siberia. *Biogeosciences*, 12, pp. 2227-2245.

Tanski, G.; Lantuit, H.; Ruttor, S.; Knoblauch, C.; Radosavljevic, B.; Strauss, J.; Wolter, J.; Irrgang, A.M.; Ramage, J. & M. Fritz (2017): Transformation of terrestrial organic matter along thermokarst-affected permafrost coasts in the Arctic. *Science of the Total Environment* 581-582, pp. 434-447.

Tarnocai, C.; Canadell, J.G.; Schuur, E.A.G.; Kuhry, P.; Mazhitova, G. & S. Zimov (2009): Soil organic carbon pools in the northern circumpolar permafrost region. *Global Biogeochem. Cycles* 23, pp. 1-11.

UNEP/GDRID-Arendal; Ahlenius, H. (2007): Permafrost extent of the Northern Hemisphere. http://www.grida.no/graphicslib/detail/permafrost-extent-in-the-northern-hemisphere_1266, (14. 10. 2017)

van Everdingen, R. (Ed.) (2005): Multi-language glossary of permafrost and related ground-ice terms. National Snow Ice Data Center/World Data Center for Glaciology, Boulder, pp. 186.

Vonk, J.E.; Sánchez-García, L.; Van Dongen, B.E.; Alling V.; Kosmach, D.; Charkin, A.; Semiletov, I.P.; Dudarev, O.V.; Shakhova, N. & P. Roos (2012): Activation of old carbon by erosion of coastal and subsea permafrost in Arctic Siberia. *Nature* 489, pp. 137-140.

Washburn, A.L. (1973): Periglacial processes and environments. London, pp. 320.

Weintraub, M.N. & J.P. Schimel (2003): Interactions between Carbon and Nitrogen Mineralization and Soil Organic Matter Chemistry in Arctic Tundra Soils. *Ecosystems* 6, pp. 129-143

Weiss, N. (2017): Permafrost carbon in a changing Arctic: On periglacial landscape dynamics, organic matter characteristics and the stability of a globally significant carbon pool. PhD thesis, University of Stockholm, pp. 55.

White, W.M. (2013): Geochemistry. Oxford, pp. 660.

Yoo, K.; Amundson, T.R.; Heimsath, A.M. & W.E. Dietrich (2006): Spatial patterns of soil organic carbon on hillslopes: Integrating geomorphic processes and the biological C cycle. *Geoderma* 130, pp. 47-65.

Young, A.; Clayton, K.M. (Ed.) (1972): Slopes. Edinburgh, pp. 288.

Zech, W.; Schad, P. & G. Hintermaier-Erhard (2014): Böden der Welt. 2nd ed., Berlin, Heidelberg, pp. 164.

Acknowledgement

A cordial thanks to all members of the COPER research group and the other colleagues at AWI Potsdam for creating a great atmosphere and making the time so appreciable.
Special thanks to Justine Ramage who always found time to answer my questions passionately even over a transatlantic distance and to Prof. Dr. Hugues Lantuit who made my time at AWI Potsdam possible! I really appreciate that all of you were able to motivate and excite me for periglacial and polar research by your helpful and candid manner and through all the conversations concerning the study.
And I want to thank Prof. Dr. Margot Böse for supporting me with expanded expertise during discussions and questions and with the cooperation between Freie Universität Berlin and Alfred-Wegener-Institute.
Finally, thanks for support and having a good time, Anna Irrgang, Simon Ploster, Maya Durstewitz, Undine Trummer and Jakob Stahl.

Appendix

1. Soil profiles for TOC, TN and C/N of every site

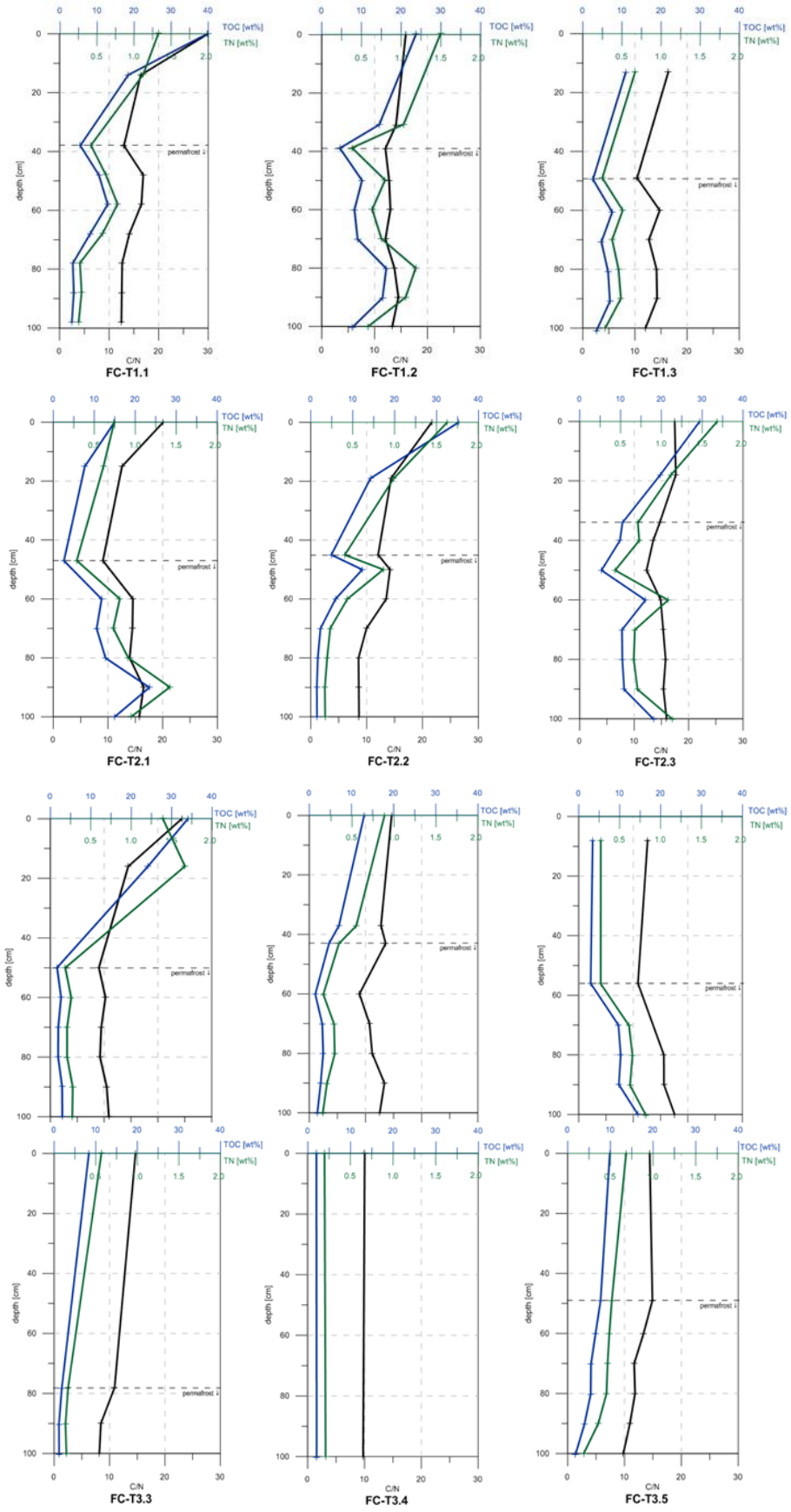

2. Boxplots for TOC, TN and C/N distribution within the active layer across the valley

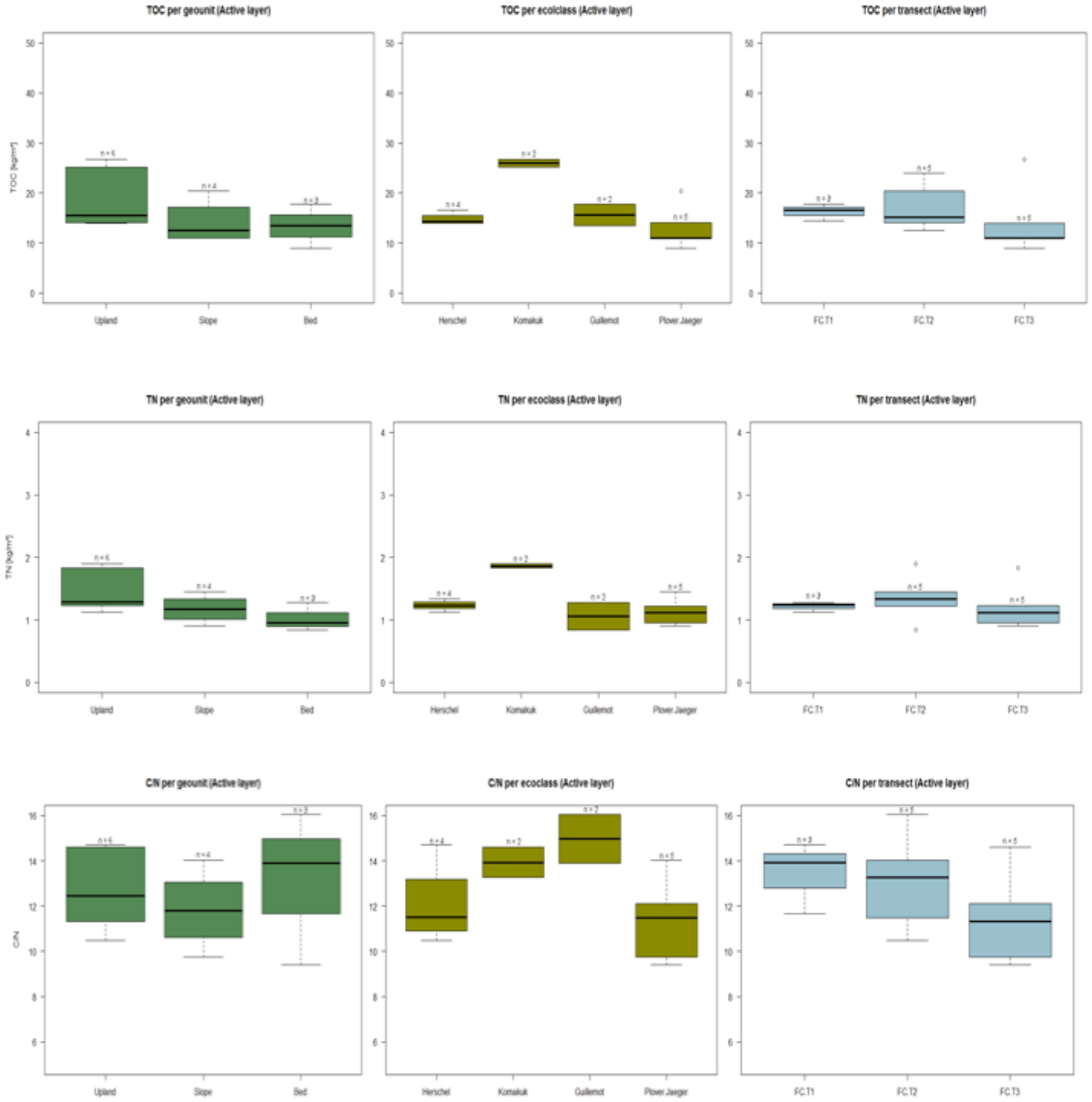

Upland (n = 6), Slope (n = 4), Bed (n =3); *Herschel* (n = 4), *Komakuk* (n = 2), *Guillemot* (n = 2), *Plover-Jaeger* (n = 5); FC-T1 (n = 3), FC-T2 (n = 5), FC-T3 (n = 5).

3. Boxplots for TOC, TN and C/N distribution within the permafrost across the valley

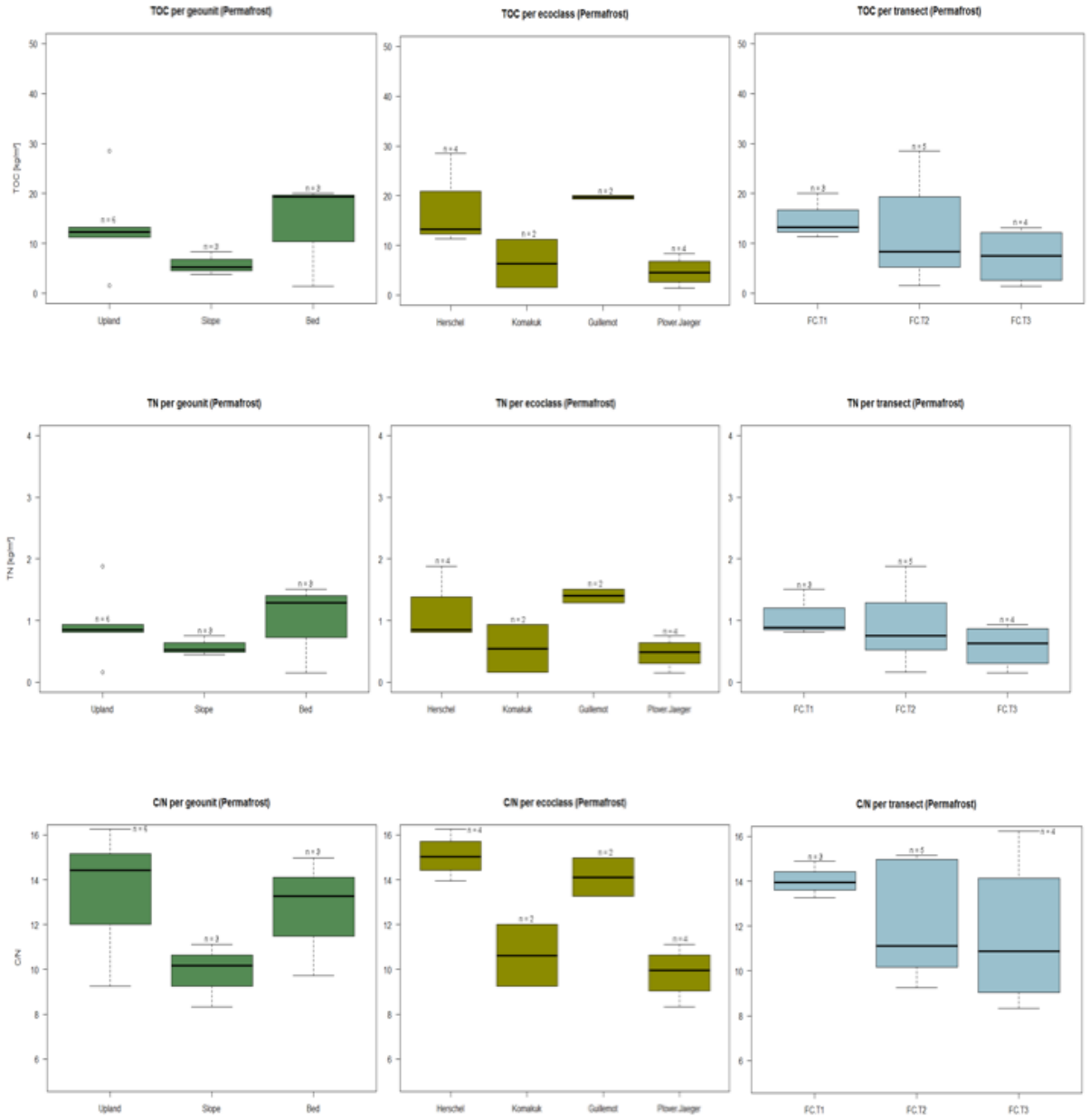

Upland (n = 6), Slope (n = 4), Bed (n =3); *Herschel* (n = 4), *Komakuk* (n = 2), *Guillemot* (n = 2), *Plover-Jaeger* (n = 5); FC-T1 (n = 3), FC-T2 (n = 5), FC-T3 (n = 4).

Sample	Definition [cm]	Elevation [m]	Geo_unit	eco_unit	frozen state	Wet weight [g]	Dry weight [g]	Water Content [g]	Volume [cm³]	Bulk Density	TN [%]	TOC [%]	sample depth [cm]	TOC storage [kg/m²]	TN storage [kg/m²]	TOC storage total [kg/m²]	TN storage total [kg/m²]	TOC storage (AL;PF) [kg/m²]	TN storage (AL;PF) [kg/m²]	C/N	C/N total	C/N (AL; PF)
FC T1.1 0-8	0-8	65,5	Upland	Herschel	0	53,30	16,33	36,97	240,00	0,07	1,328	39,766	8	2,165	0,072					29,9		
FC T1.1 8-14	8-14	65,5	Upland	Herschel	0	206,35	79,97	126,38	235,50	0,34	1,123	18,404	6	3,750	0,229					16,4		
FC-T1.1 14-38	14-38	65,5	Upland	Herschel	0	286,03	193,03	93,00	235,50	0,82	0,419	5,449	24	10,719	0,825			16,630	1,130	13,0		14,7
FC-T1.1 38-48	38-48	65,5	Upland	Herschel	1	29,26	49,10	-19,84	145,22	0,34	0,619	10,458	10	3,536	0,209					16,9		
FC-T1.1 48-58	48-58	65,5	Upland	Herschel	1	114,01	35,80	78,21	145,22	0,25	0,778	12,850	10	3,168	0,192					16,5		
FC-T1.1 58-68	58-68	65,5	Upland	Herschel	1	146,68	60,20	86,48	145,22	0,41	0,576	8,112	10	3,363	0,239					14,1		
FC-T1.1 68-78	68-78	65,5	Upland	Herschel	1	145,56	48,10	97,46	145,22	0,33	0,271	3,426	10	1,135	0,090					12,6		
FC-T1.1 78-88	78-88	65,5	Upland	Herschel	1	148,66	47,20	101,46	145,22	0,33	0,293	3,680	10	1,196	0,095					12,6		
FC-T1.1 88-98	88-98	65,5	Upland	Herschel	1	110,57	38,90	71,67	145,22	0,27	0,254	3,174	10	0,850	0,068	29,881	2,020	13,250	0,890	12,5	14,8	14,9
FC-T1.1 98-100	98-100	65,5	Upland	Herschel	1	1	1	NA	NA	NA	NA	NA	2									
FC-T1.2 0-10	0-10	62,2	Bed	Guillemot	0	79,29	15,93	63,36	122,50	0,13	1,497	23,789	10	3,094	0,195					15,9		
FC-T1.2 10-31	10-31	62,2	Bed	Guillemot	0	251,93	90,63	161,30	235,50	0,38	1,030	14,474	21	11,697	0,833					14,0		
FC-T1.2 31-39	31-39	62,2	Bed	Guillemot	0	286,66	194,03	92,63	235,50	0,82	0,380	4,577	8	3,017	0,251			17,810	1,280	12,0		13,9
FC-T1.2 39-50	39-50	62,2	Bed	Guillemot	1	155,66	57,90	97,76	145,22	0,40	0,797	10,157	11	4,455	0,349					12,7		
FC-T1.2 50-60	50-60	62,2	Bed	Guillemot	1	136,41	30,40	106,01	145,22	0,21	0,635	8,246	10	1,726	0,133					13,0		
FC-T1.2 60-70	60-70	62,2	Bed	Guillemot	1	122,38	49,30	73,08	145,22	0,34	0,751	9,045	10	3,071	0,255					12,0		
FC-T1.2 70-80	70-80	62,2	Bed	Guillemot	1	119,92	34,30	85,62	145,22	0,24	1,183	16,251	10	3,838	0,279					13,7		
FC-T1.2 80-90	80-90	62,2	Bed	Guillemot	1	143,72	46,20	97,52	145,22	0,32	1,056	15,308	10	4,870	0,336					14,5		
FC-T1.2 90-100	90-100	62,2	Bed	Guillemot	1	137,29	38,70	98,59	145,22	0,27	0,581	7,750	10	2,065	0,155	37,833	2,790	20,030	1,510	13,3	13,6	13,3
FC-T1.3 0-3	0-3	66,5	Upland	Herschel	0	NA	NA	NA	NA	NA	NA	NA	3									
FC-T1.3 3-13	3-13	66,5	Upland	Herschel	0	201,60	92,97	108,63	235,50	0,39	0,668	10,949	10	4,323	0,264					16,4		
FC-T1.3 13-49	13-49	66,5	Upland	Herschel	0	330,19	256,03	74,16	235,50	1,09	0,249	2,594	36	10,151	0,975			14,470	1,240	10,4		11,7

Sample	Definition [cm]	Elevation [m]	Geo_unit	eco_unit	frozen state	Wet weight [g]	Dry weight [g]	Water Content [g]	Volume [cm³]	Bulk Density	TN [%]	TOC [%]	sample depth [cm]	TOC storage [kg/m²]	TN storage [kg/m²]	TOC storage total [kg/m²]	TN storage total [kg/m²]	TOC storage (AL;PF) [kg/m²]	TN storage (AL;PF) [kg/m²]	C/N	C/N total	C/N (AL; PF)
FC-T1.3 49-60	49-60	66,5	Upland	Herschel	1	162,71	68,03	94,68	145,22	0,47	0,509	7,510	11	3,870	0,263					14,7		
FC-T1.3 60-70	60-70	66,5	Upland	Herschel	1	129,21	51,53	77,68	145,22	0,35	0,375	4,747	10	1,684	0,133					12,7		
FC-T1.3 70-80	70-80	66,5	Upland	Herschel	1	165,65	60,33	105,32	145,22	0,42	0,456	6,438	10	2,675	0,189					14,1		
FC-T1.3 80-90	80-90	66,5	Upland	Herschel	1	161,45	50,50	110,95	145,22	0,35	0,486	6,918	10	2,406	0,169					14,2		
FC-T1.3 90-100	90-100	66,5	Upland	Herschel	1	136,90	27,60	109,30	145,22	0,19	0,287	3,442	10	0,654	0,054	25,763	2,050	11,290	0,810	12,0	12,6	13,9
FC-T2.1 0-6	0-6	67,9	Upland	Herschel	0	53,15	26,37	26,78	156,00	0,17	0,743	14,921	6	1,513	0,075					20,1		
FC-T2.1 6-15	6-15	67,9	Upland	Herschel	0	237,01	135,73	101,28	235,50	0,58	0,612	7,683	9	3,985	0,317					12,6		
FC-T2.1 15-47	15-47	67,9	Upland	Herschel	0	321,17	243,17	78,00	235,50	1,03	0,286	2,590	32	8,556	0,944			14,060	1,340	9,1		10,5
FC-T2.1 47-60	47-60	67,9	Upland	Herschel	1	175,92	76,57	99,35	145,22	0,53	0,811	11,792	13	8,083	0,556					14,5		
FC-T2.1 60-70	60-70	67,9	Upland	Herschel	1	104,45	39,57	64,88	145,22	0,27	0,731	10,576	10	2,882	0,199					14,5		
FC-T2.1 70-80	70-80	67,9	Upland	Herschel	1	147,53	42,17	105,36	145,22	0,29	0,913	12,747	10	3,702	0,265					14,0		
FC-T2.1 80-90	80-90	67,9	Upland	Herschel	1	135,14	43,27	91,87	145,22	0,30	1,420	23,446	10	6,986	0,423					16,5		
FC-T2.1 90-100	90-100	67,9	Upland	Herschel	1	142,38	66,60	75,78	145,22	0,46	0,952	14,963	10	6,862	0,437	42,570	3,220	28,520	1,880	15,7	13,2	15,2
FC-T2.2 0-8	0-8	63,4	Slope	Plover-Jaeger	0	36,60	15,4	21,88	105,00	0,15	1,629	35,269	8	4,138	0,191					21,6		
FC-T2.2 8-19	8-19	63,4	Slope	Plover-Jaeger	0	195,17	95,82	99,35	235,50	0,41	0,991	14,250	11	6,378	0,444					14,4		
FC-T2.2 19-45	19-45	63,4	Slope	Plover-Jaeger	0	244,24	181,9	63,02	235,50	0,77	0,406	4,892	26	9,824	0,815			20,340	1,450	12,1		14,0
FC-T2.2 45-50	45-50	63,4	Slope	Plover-Jaeger	1	77,15	31,65	42,03	145,22	0,22	0,865	12,268	5	1,337	0,094					14,2		
FC-T2.2 50-60	50-60	63,4	Slope	Plover-Jaeger	1	169,97	82,12	87,85	145,22	0,57	0,436	5,890	10	3,331	0,247					13,5		
FC-T2.2 60-70	60-70	63,4	Slope	Plover-Jaeger	1	156,05	65,75	86,83	145,22	0,45	0,231	2,307	10	1,045	0,105					10,0		
FC-T2.2 70-80	70-80	63,4	Slope	Plover-Jaeger	1	155,37	88,95	62,95	145,22	0,61	0,195	1,666	10	1,020	0,120					8,5		

Sample	Definition [cm]	Elevation [m]	Geo_unit	eco_unit	frozen state	Wet weight [g]	Dry weight [g]	Water Content [g]	Volume [cm³]	Bulk Density	TN [%]	TOC [%]	sample depth [cm]	TOC storage [kg/m²]	TN storage [kg/m²]	TOC storage total [kg/m²]	TN storage total [kg/m²]	TOC storage (AL;PF) [kg/m²]	TN storage (AL;PF) [kg/m²]	C/N	C/N total	C/N (AL; PF)
FC-T2.2 80-90	80-90	63,4	Slope	Plover-Jaeger	1	124,83	69,37	55,46	145,22	0,48	0,168	1,444	10	0,690	0,080					8,6		
FC-T2.2 90-100	90-100	63,4	Slope	Plover-Jaeger	1	153,53	89,32	64,21	145,22	0,62	0,171	1,476	10	0,908	0,105	28,671	2,200	8,330	0,750	8,6	13,0	11,1
FC-T2.3 0-8	0-8	56,2	Bed	Guillemot	0	80,36	16,67	63,69	120,00	0,14	1,684	29,373	8	3,264	0,187					17,4		
FC-T2.3 8-18	8-18	56,2	Bed	Guillemot	0	189,08	42,53	146,55	235,50	0,18	1,116	19,696	10	3,557	0,202					17,6		
FC-T2.3 18-34	18-34	56,2	Bed	Guillemot	0	245,22	93,73	151,49	235,50	0,40	0,712	10,469	16	6,667	0,453			13,490	0,840	14,7		16,1
FC-T2.3 34-40	34-40	56,2	Bed	Guillemot	1	133,54	68,77	64,77	145,22	0,47	0,729	9,837	6	2,795	0,207					13,5		
FC-T2.3 40-50	40-50	56,2	Bed	Guillemot	1	57,90	30,17	27,73	145,22	0,21	0,434	5,326	10	1,107	0,090					12,3		
FC-T2.3 50-60	50-60	56,2	Bed	Guillemot	1	118,34	24,50	93,84	145,22	0,17	1,082	16,085	10	2,714	0,183					14,9		
FC-T2.3 60-70	60-70	56,2	Bed	Guillemot	1	164,10	45,40	118,70	145,22	0,31	0,675	10,350	10	3,236	0,211					15,3		
FC-T2.3 70-80	70-80	56,2	Bed	Guillemot	1	131,48	36,60	94,88	145,22	0,25	0,662	10,438	10	2,631	0,167					15,8		
FC-T2.3 80-90	80-90	56,2	Bed	Guillemot	1	126,00	28,20	97,80	145,22	0,19	0,708	10,888	10	2,114	0,138					15,4		
FC-T2.3 90-100	90-100	56,2	Bed	Guillemot	1	171,90	38,00	133,90	145,22	0,26	1,135	18,097	10	4,736	0,297	32,820	2,130	19,330	1,290	15,9	15,4	15,0
FC-T2.4 0-7	0-7	60,1	Slope	Plover-Jaeger	0	31,92	10,63	21,29	235,50	0,05	1,391	34,012	7	1,075	0,044					24,5		
FC-T2.4 7-16	7-16	60,1	Slope	Plover-Jaeger	0	223,55	66,53	157,02	235,50	0,28	1,666	24,123	9	6,133	0,424					14,5		
FC-T2.4 16-50	16-49	60,1	Slope	Plover-Jaeger	0	349,56	283,03	66,53	235,50	1,20	0,185	1,665	34	6,802	0,754			14,010	1,220	9,0		11,5

Sample	Definition [cm]	Elevation [m]	Geo_unit	eco_unit	frozen state	Wet weight [g]	Dry weight [g]	Water Content [g]	Volume [cm³]	Bulk Density	TN [%]	TOC [%]	sample depth [cm]	TOC storage [kg/m²]	TN storage [kg/m²]	TOC storage total [kg/m²]	TN storage total [kg/m²]	TOC storage (AL;PF) [kg/m²]	TN storage (AL;PF) [kg/m²]	C/N	C/N total	C/N (AL; PF)
FC-T2.4 50-60	50-60	60,1	Slope	Plover-Jaeger	1	138,12	62,47	75,65	145,22	0,43	0,258	2,645	10	1,138	0,111					10,2		
FC-T2.4 60-70	60-70	60,1	Slope	Plover-Jaeger	1	145,20	34,67	110,53	145,22	0,24	0,207	1,955	10	0,467	0,049					9,5		
FC-T2.4 70-80	70-80	60,1	Slope	Plover-Jaeger	1	158,53	66,87	91,66	145,22	0,46	0,208	1,919	10	0,883	0,096					9,2		
FC-T2.4 80-90	80-90	60,1	Slope	Plover-Jaeger	1	162,11	63,32	98,79	145,22	0,44	0,277	2,904	10	1,266	0,121					10,5		
FC-T2.4 90-100	90-100	60,1	Slope	Plover-Jaeger	1	152,93	75,62	77,31	145,22	0,52	0,271	2,951	10	1,536	0,141	19,301	1,740	5,290	0,520	10,9	11,1	10,2
FC-T2.5 0-9	0-9	71,3	Upland	Komakuk	0	112,59	52,63	59,96	135,00	0,39	0,887	13,001	9	4,562	0,311					14,7		
FC-T2.5 9-37	22-28	71,3	Upland	Komakuk	0	257,47	166,37	91,10	235,50	0,71	0,551	7,024	28	13,895	1,089					12,8		
FC-T2.5 37-50	37-43	71,3	Upland	Komakuk	0	242,63	261,37	-18,74	235,50	1,11	0,344	4,669	13	6,737	0,496			25,190	1,900	13,6		13,3
FC-T2.5 50-60	50-60	71,3	Upland	Komakuk	1	200,40	133,47	66,93	145,22	0,92	0,158	1,411	10	1,297	0,145					8,9		
FC-T2.5 60-70	60-70	71,3	Upland	Komakuk	1	124,56	4,27	120,29	145,22	0,03	0,287	3,071	10	0,090	0,008					10,7		
FC-T2.5 70-80	70-80	71,3	Upland	Komakuk	1	22,52	1,37	21,15	145,22	0,01	0,294	3,289	10	0,031	0,003					11,2		
FC-T2.5 80-90	80-90	71,3	Upland	Komakuk	1	7,45	2,87	4,58	145,22	0,02	0,201	2,688	10	0,053	0,004					13,4		
FC-T2.5 90-100	90-100	71,3	Upland	Komakuk	1	9,39	0,77	8,62	145,22	0,01	0,151	1,898	10	0,010	0,001	26,675	2,060	1,480	0,160	12,5	12,9	9,3
FC-T3.1 0-1	0-1	59,3	Upland	Herschel	0	NA	NA	NA	NA	NA	NA	NA	NA									
FC-T3.1 1-8	1-8	59,3	Upland	Herschel	0	254,87	190,27	64,60	235,50	0,81	0,269	3,400	7	1,923	0,152					12,6		

Sample	Definition [cm]	Elevation [m]	Geo_unit	eco_unit	frozen state	Wet weight [g]	Dry weight [g]	Water Content [g]	Volume [cm³]	Bulk Density	TN [%]	TOC [%]	sample depth [cm]	TOC storage [kg/m²]	TN storage [kg/m²]	TOC storage total [kg/m²]	TN storage total [kg/m²]	TOC storage (AL;PF) [kg/m²]	TN storage (AL;PF) [kg/m²]	C/N	C/N total	C/N (AL; PF)
FC-T3.1 8-56	8-56	59,3	Upland	Herschel	0	267,98	197,37	70,61	235,50	0,84	0,269	2,917	48	11,734	1,081			13,930	1,230	10,9		11,3
FC-T3.1 56-70	56-70	59,3	Upland	Herschel	1	140,80	NA	NA	145,22	NA	0,615	9,695	14									
FC-T3.1 70-80	70-80	59,3	Upland	Herschel	1	121,91	42,07	79,84	145,22	0,29	0,657	10,252	10	2,970	0,190					15,6		
FC-T3.1 80-90	80-90	59,3	Upland	Herschel	1	227,42	93,87	133,55	145,22	0,65	0,627	9,800	10	6,335	0,405					15,6		
FC-T3.1 90-100	90-100	59,3	Upland	Herschel	1	135,28	38,77	96,51	145,22	0,27	0,821	14,437	10	3,854	0,219	26,817	2,050	13,160	0,810	17,6		16,2
FC-T3.2 1-86	1-86	51,4	Bed	Plover-Jaeger	0	NA	NA	NA	NA	NA	NA	NA	NA		0,951			8,940	0,950	0,0		9,4
FC-T3.2 86-100	86-100	51,4	Bed	Plover-Jaeger	1	98,76	98,72	0,04	145,22	0,68	0,163	1,529	14	1,455	0,155	1,455	1,110	1,460	0,150	9,4	1,3	9,7
FC-T3.3 0-9	0-9	46,3	Slope	Plover-Jaeger	0	166,41	130,82	35,59	235,50	0,56	0,568	8,346	9	4,172	0,284					14,7		
FC-T3.3 9-78	9-78	46,3	Slope	Plover-Jaeger	0	201,42	127,67	73,75	235,50	0,54	0,168	1,829	69	6,843	0,627			11,020	0,910	10,9		12,1
FC-T3.3 78-90	78-90	46,3	Slope	Plover-Jaeger	1	366,35	289,47	76,88	145,22	1,99	0,136	1,148	12	2,746	0,326					8,4		
FC-T3.3 90-100	90-100	46,3	Slope	Plover-Jaeger	1	188,91	122,27	66,64	145,22	0,84	0,147	1,196	10	1,007	0,124	14,768	1,360	3,750	0,450	8,2	10,9	8,3
FC-T3.4 0-12	0-12	42,2	Slope	Plover-Jaeger	0	188,19	125,87	62,32	235,50	0,53	0,197	1,980	12	1,270	0,126					10,0		
FC-T3.4 12-100	12-100	42,2	Slope	Plover-Jaeger	0	155,81	126,21	29,60	235,50	0,54	0,210	2,048	88	9,659	0,990	10,928	1,120	10,930	1,120	9,8	9,8	9,8
FC-T3.5 0-14	0-14	47,6	Upland	Komakuk	0	317,91	261,89	56,02	235,50	1,11	0,684	9,871	14	15,368	1,065					14,4		
FC-T3.5 14-49	14-49	47,6	Upland	Komakuk	0	140,24	99,12	41,12	235,50	0,42	0,517	7,702	35	11,346	0,761			26,710	1,830	14,9		14,6

Sample	Definition [cm]	Elevation [m]	Geo_unit	eco_unit	frozen state	Wet weight [g]	Dry weight [g]	Water Content [g]	Volume [cm³]	Bulk Density	TN [%]	TOC [%]	sample depth [cm]	TOC storage [kg/m²]	TN storage [kg/m²]	TOC storage total [kg/m²]	TN storage total [kg/m²]	TOC storage (AL;PF) [kg/m²]	TN storage (AL;PF) [kg/m²]	C/N	C/N total	C/N (AL; PF)
FC-T3.5 49-60	49-60	47,6	Upland	Komakuk	1	156,52	96,67	59,85	145,22	0,67	0,488	6,514	11	4,770	0,357					13,3		
FC-T3.5 60-70	60-70	47,6	Upland	Komakuk	1	150,38	73,02	77,36	145,22	0,50	0,467	5,470	10	2,750	0,235					11,7		
FC-T3.5 70-80	70-80	47,6	Upland	Komakuk	1	168,03	41,52	126,51	145,22	0,29	0,455	5,394	10	1,542	0,130					11,9		
FC-T3.5 80-90	80-90	47,6	Upland	Komakuk	1	111,37	39,57	71,80	145,22	0,27	0,359	3,928	10	1,070	0,098					10,9		
FC-T3.5 90-100	90-100	47,6	Upland	Komakuk	1	200,34	81,22	119,12	145,22	0,56	0,188	1,839	10	1,028	0,105	37,876	2,750	11,160	0,930	9,8	13,8	12,0

5. R Skript Statistical analysis

```
# by different sessions

# correlations test for TOC TN CN total with active layer depth

data1 <- read.csv(file.choose(), header=T, sep=";")
cor(data1)
          TOC         TN       C.N.      Depth
TOC    1.0000000  0.9777684  0.8386143 -0.8113470
TN     0.9777684  1.0000000  0.7139348 -0.7429226
C.N.   0.8386143  0.7139348  1.0000000 -0.8858842
Depth -0.8113470 -0.7429226 -0.8858842  1.0000000

#correlations test for TOC TN CN of active layer with active layer depth

data2 <- read.csv(file.choose(), header=T, sep=",")
cor(data2)
Depth       TOC.        TN.       C.N.
Depth  1.0000000 -0.5659921 -0.3449338 -0.7479924
TOC.  -0.5659921  1.0000000  0.9070102  0.5916828
TN.   -0.3449338  0.9070102  1.0000000  0.2064247
C.N.  -0.7479924  0.5916828  0.2064247  1.0000000


#test of normal distribution wit shapiro.test for C/N ratio geounits
#Shapiro-Wilk normality test

shapiro.test(data1$Upland)
W = 0.9095, p-value = 0.433    -> p > 0.05 ->  Values underlie normal distribution
shapiro.test(data1$Slope)
data:  data1$Slope
W = 0.9419, p-value = 0.6662   -> p > 0.05 ->  Values underlie normal distribution
shapiro.test(data1$Bed)
data:  data1$Bed
W = 0.9521, p-value = 0.5787   -> p > 0.05 ->  Values underlie normal distribution


#test of normal distribution wit shapiro.test for C/N ratio transects
data2 <- read.csv(file.choose(), header=T. sep=",")
shapiro.test(data2$FC.T1)
data:  data2$FC.T1
W = 0.9962, p-value = 0.8816    -> p > 0.05 ->  Values underlie normal distribution
shapiro.test(data2$FC.T2)
data:  data2$FC.T2
W = 0.9165, p-value = 0.5078    -> p > 0.05 ->  Values underlie normal distribution
shapiro.test(data2$FC.T3)
data:  data2$FC.T3
W = 0.8824, p-value = 0.3203    -> p > 0.05 ->  Values underlie normal distribution

#test of normal distribution wit shapiro.test for C/N ratio ecoclass
data3 <- read.csv(file.choose(), header=T, sep=",")
shapiro.test(data3$Herschel)
data:  data3$Herschel
W = 0.8707, p-value = 0.3004    -> p > 0.05 ->  Values underlie normal distribution
> shapiro.test(data3$Komakuk)
Error in shapiro.test(data3$Komakuk) :
  Stichprobengröße muss zwischen 3 und 5000 liegen  -> only 2 values
> shapiro.test(data3$Guillemot)
Error in shapiro.test(data3$Guillemot) :
  Stichprobengröße muss zwischen 3 und 5000 liegen  -> only 2 values
> shapiro.test(data3$Plover.Jaeger)
data:  data3$Plover.Jaeger
W = 0.9269, p-value = 0.5756    -> p > 0.05 ->  Values underlie normal distribution



#significance test ANOVA
```

```
CN_geounit <- read.csv(file.choose(), header=F, sep=";")

anova(lm(CN_geounit$V2 ~ CN_geounit$V1))

Analysis of Variance Table

Response: CN_geounit$V2
             Df Sum Sq Mean Sq F value Pr(>F)
CN_geounit$V1  2 12.137  6.0687  2.1889 0.1628
Residuals     10 27.726  2.7726                   -> no significance!

- significance codes: Signif. codes:  0 '***' 0.001 '**' 0.01 '*' 0.05 '.' 0.1 ' '
1

CN_transect <- read.csv(file.choose(), header=F, sep=";")
anova(lm(CN_transect$V2 ~ CN_transect$V1))
Response: CN_transect$V2
               Df Sum Sq Mean Sq F value Pr(>F)
CN_transect$V1  2 11.948  5.9739    2.14 0.1684
Residuals      10 27.915  2.7915                     -> no significance!

CN_ecoclass <- read.csv(file.choose(), header=F, sep=";")
anova(lm(CN_ecoclass$V2 ~CN_ecoclass$V1))
Response: CN_ecoclass$V2
               Df Sum Sq Mean Sq F value  Pr(>F)
CN_ecoclass$V1  3 26.955  8.9850  6.2648 0.01387 *    signiciance!
  Residuals       9 12.908  1.4342
---
  Signif. codes:  0 '***' 0.001 '**' 0.01 '*' 0.05 '.' 0.1 ' ' 1

#ANOVA shows a significant differences between the mean values of the 4 groups of
ecoclasses! Herschel u. Plover-Jaeger p < 0.05

t.test(data3$Herschel,data3$Plover.Jaeger)
Welch Two Sample t-test

data:  data3$Herschel and data3$Plover.Jaeger
t = 3.2977, df = 6.841, p-value = 0.0136
alternative hypothesis: true difference in means is not equal to 0    -> p value <
0.05 -> fail to reject H0 -> dataset statistically significant!
  95 percent confidence interval:
  0.734558 4.520854
sample estimates:
  mean of x mean of y
13.44896  10.82125


# R Script boxplot

data2 <- read.csv(file.choose(),header=T)
boxplot(data2, main="TOC per geounit", ylab="TOC [kg/m²]", ylim=c(0, 50), las=1,
col = c("palegreen4","palegreen4","palegreen4"))

data3 <- read.csv(file.choose(),header=T)
boxplot(data3)
boxplot(data3, main="TN per geounit", ylab="TN [kg/m²]", ylim=c(0, 4), las=1, col =
c("palegreen4","palegreen4","palegreen4"))
data4 <- read.csv(file.choose(),header=T)
boxplot(data4, main="C/N per geounit", ylab="C/N", ylim=c(0, 16), las=1, col =
c("palegreen4","palegreen4","palegreen4"))

boxplot(data4, main="C/N per geounit", ylab="C/N", ylim=c(5, 15), las=1, col =
c("palegreen4","palegreen4","palegreen4"))

boxplot(data4, main="C/N per geounit", ylab="C/N", ylim=c(5, 16), las=1, col =
c("palegreen4","palegreen4","palegreen4"))

data5 <- read.csv(file.choose(), header=T)
```

```
boxplot(data5, main="TOC per transect", ylab="TOC [kg/m²]", ylim=c(0, 50), las=1,
col = c("lightblue3","lightblue3","lightblue3"))

data6 <- read.csv(file.choose(), header=T)
boxplot(data6, main="TN per transect", ylab="TN [kg/m²]", ylim=c(0, 4), las=1, col
= c("lightblue3","lightblue3","lightblue3"))

data7 <- read.csv(file.choose(), header=T)
boxplot(data7, main="C/N per transect", ylab="C/N", ylim=c(5, 16), las=1, col =
c("lightblue3","lightblue3","lightblue3"))

data8 <- read.csv(file.choose(), header=T)
boxplot(data8, main="TOC per ecoclass", ylab="TOC [kg/m²]", ylim=c(0, 50), las=1,
col = c("yellow4","yellow4","yellow4"))

data9 <- read.csv(file.choose(), header=T)
boxplot(data9, main="TN per ecoclass", ylab="TN [kg/m²]", ylim=c(0, 4), las=1, col
= c("yellow4","yellow4","yellow4"))

data10 <- read.csv(file.choose(), header=T)
boxplot(data10, main="C/N per ecoclass", ylab="C/N", ylim=c(5, 16), las=1, col =
c("yellow4","yellow4","yellow4"))
```

Eidgenössische Erklärung

Hiermit bestätige ich, dass diese Arbeit eigenständig von mir verfasst wurde und frei von Plagiaten ist. Es wurden zur Anfertigung der Arbeit ausschließlich die angegebenen Quellen genutzt und ordnungsgemäß zitiert.

Berlin, 24.11.2017 _____

Luca Durstewitz